(12) INTERNATIONAL APPLICATION PUBLISHED UNDER THE PATENT COOPERATION TREATY (PCT)

(19) World Intellectual Property Organization
International Bureau

(43) International Publication Date
30 March 2017 (30.03.2017)

WIPO | PCT

(10) International Publication Number
WO 2017/053522 A1

(51) International Patent Classification:
G01C 23/00 (2006.01)

(21) International Application Number:
PCT/US2016/053030

(22) International Filing Date:
22 September 2016 (22.09.2016)

(25) Filing Language: English

(26) Publication Language: English

(30) Priority Data:
62/221,858 22 September 2015 (22.09.2015) US

(71) Applicant: **OHIO UNIVERSITY** [US/US]; 340 West State Street, Unit 14, Athens, OH 45701-2979 (US).

(72) Inventors: **ZHU, Jianchao**; 7386 Whitland Lane, Athens, OH 45701 (US). **ZHAO, Yue**; 1003 Carriage Hill Drive, Athens, OH 45701 (US).

(74) Agents: **BLATT, P., Andrew** et al.; Wood Herron & Evans LLP, 441 Vine Street, Suite 2700, Cincinnati, OH 45202-2917 (US).

(81) Designated States *(unless otherwise indicated, for every kind of national protection available)*: AE, AG, AL, AM, AO, AT, AU, AZ, BA, BB, BG, BH, BN, BR, BW, BY, BZ, CA, CH, CL, CN, CO, CR, CU, CZ, DE, DK, DM, DO, DZ, EC, EE, EG, ES, FI, GB, GD, GE, GH, GM, GT, HN, HR, HU, ID, IL, IN, IR, IS, JP, KE, KG, KN, KP, KR, KW, KZ, LA, LC, LK, LR, LS, LU, LY, MA, MD, ME, MG, MK, MN, MW, MX, MY, MZ, NA, NG, NI, NO, NZ, OM, PA, PE, PG, PH, PL, PT, QA, RO, RS, RU, RW, SA, SC, SD, SE, SG, SK, SL, SM, ST, SV, SY, TH, TJ, TM, TN, TR, TT, TZ, UA, UG, US, UZ, VC, VN, ZA, ZM, ZW.

(84) Designated States *(unless otherwise indicated, for every kind of regional protection available)*: ARIPO (BW, GH, GM, KE, LR, LS, MW, MZ, NA, RW, SD, SL, ST, SZ, TZ, UG, ZM, ZW), Eurasian (AM, AZ, BY, KG, KZ, RU, TJ, TM), European (AL, AT, BE, BG, CH, CY, CZ, DE, DK, EE, ES, FI, FR, GB, GR, HR, HU, IE, IS, IT, LT, LU, LV, MC, MK, MT, NL, NO, PL, PT, RO, RS, SE, SI, SK, SM, TR), OAPI (BF, BJ, CF, CG, CI, CM, GA, GN, GQ, GW, KM, ML, MR, NE, SN, TD, TG).

Published:

— *with international search report (Art. 21(3))*

WO 2017/053522 A1

(54) Title: LOSS-OF-CONTROL PREVENTION AND RECOVERY FLIGHT CONTROLLER

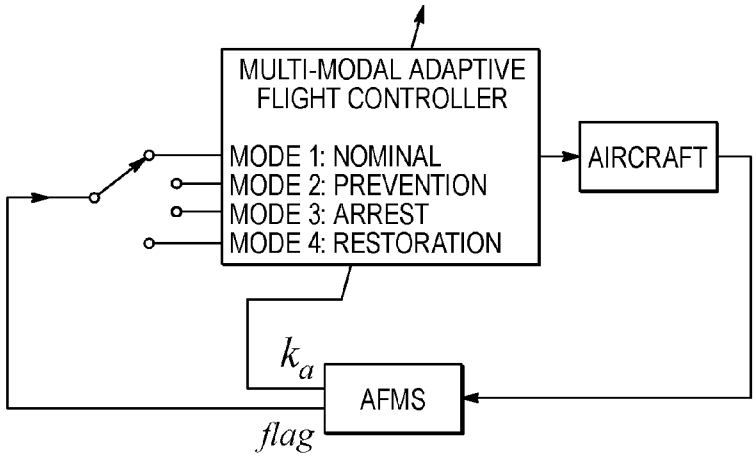


FIG. 14

(57) Abstract: A loss-of-control prevention and recovery automatic control system of an aircraft is provided having a plurality of flight control mode, including a nominal flight control mode, a loss-of-control prevention control mode, a loss-of-control arrest control mode, and a nominal flight restoration control mode, as well as a supervisory control system capable of monitoring the flight states and flight events of the aircraft and determining which flight control mode to activate.

LOSS-OF-CONTROL PREVENTION AND RECOVERY FLIGHT CONTROLLER

Cross-Reference to Related Application

[0001] This application claims priority to U.S. Provisional Patent Application Serial No. 62/221,858, filed on September 22, 2015, the disclosure of which is incorporated by reference herein in its entirety.

Technical Field

[0002] The present invention relates generally to a flight control system for fixed-wing aircraft, and more specifically a hybrid flight control system for loss-of-control prevention and recovery.

Background

[0003] There are three types of forces acting on an airplane simultaneously: the aerodynamic force, the gravitational force, and the propulsion. The aerodynamic force has three components: lift force, drag force, and side force. These forces are generated by the relative motion of the airfoil with respect to the atmosphere. Since dependencies of aerodynamic forces are usually very complex, approximations are made to determine the aerodynamic force by aerodynamic angles including angle-of-attack, side-slip angle, and bank angle.

[0004] Angle-of-attack can be defined as the angle between the wing airfoil chord line and the relative wind. In normal operations, the lift is directly proportional to angle-of-attack. However, angle-of-attack cannot exceed an upper bound which is called the critical angle-of-attack, since beyond it flow separation induced stall may occur causing sudden reduction of the lift. In the situation of the stall, the airplane will lose altitude and the ability to control its attitude. The side-slip angle is the angle between the oncoming airflow and the direction towards which the aircraft is pointing. Similar to the angle-of-attack, side-slip angle determines the magnitude of side force. The large side-slip angle may cause severe vibration of propellers or surge in turbo-engines, which may lead to Loss-of-Control ("LOC") or cause damage to the vehicle. Large side-slip angles combined with a stall may induce lateral spins of the aircraft which may not be recoverable. Side slipping is undesirable since a lateral acceleration directed toward the airplane center makes passengers uncomfortable. Bank angle is the angle of the vehicle longitudinal axis inclines with respect to its velocity vector. It is a preferred maneuver in carrying out a turn, known as a Bank-to-Turn (BTT). If the vehicle is

overbanked, it may lose altitude and go into a spiral dive due to inadequate lift. Therefore, the pilot or autopilot would lose the ability to fix the aircraft with the aerodynamic angles exceeding the safety boundaries, causing the vehicle to go into LOC. Here LOC means that the pilot would not be able to operate the plane, even though the control system of the aircraft may still be physically intact and functional.

[0005] Based on the Airplane Upset Recovery Training Aid provided by the Federal Aviation Administration (FAA), "an airplane in flight unintentionally exceeding the parameters normally experienced in operations or training" is called airplane upset. LOC is described as motions that are: 1) outside the normal operating flight envelopes; 2) not predictably controlled by pilot inputs; 3) high angular rates and displacements. Statistics of airplane accidents show that aircraft LOC were associated with aircraft component failures (including jammed control surfaces, loss of engines, icing contamination), weather conditions (including turbulence, wind shear, mountain waves), and inappropriate crew control. The analysis also shows that the LOC accidents usually involve more than one contributing factor and consequently drive the aircraft into an inadvertent event with abnormal aircraft attitude, angular rate, acceleration, airspeed, or flight trajectory.

[0006] According to the statistical report of commercial jet accidents occurring from 2003 through 2012 created by the Boeing Company, LOC-in-flight was the number one cause in terms of both the number of accidents and the number of fatalities. There were 18 accidents and 1,648 deaths caused by LOC during that period. Moreover, not only for commercial transport airplanes, LOC is listed to be the number one cause of upset events also for general aviation.

[0007] Thus, the Commercial Aviation Safety Team (CAST) has spearheaded the effort to define the causes of LOC and to develop interventions to prevent these accidents. Even though the automatic flight control system (autopilot) is usually equipped in modern aircraft operation systems to reduce the pilot's workload, the FAA upset recovery rules still require that the pilot needs to take control of the aircraft when LOC occurs. Several pilot training programs provide simulators to educate pilots so that they will have adequate skills to prevent and recover from upsets. Because pilot recovery depends on the pilot response time and may involve inappropriate operations due to human errors, it would be beneficial to develop effective interventions by designing an automatic system that has the capabilities of correctly and promptly responding to unanticipated events and recover from adverse LOC situations.

[0008] The chain of complex events that cause LOC and proper interventions can be subdivided into nominal, prevention, LOC arrest, and mission restoration. Prevention is defined to be the control strategies and maneuvers to sustain normal flight under unexpected adverse events such as environmental hazards, system failures, vehicle damage, or pilot errors. In the event that prevention fails and the aircraft still slips into upset situations, then LOC arrest becomes necessary, which is to activate control strategies to rescue the aircraft from a LOC event. A stabilized flight path recovery should be initiated as soon as LOC arrest maneuvers are complete, which is the restoration. LOC arrest and restoration will eventually achieve full flight mission recovery.

[0009] In the past, small wind disturbance accommodation has been considered in the aircraft control system design, but advanced aircraft control method should be applied for control system design to improve the robustness so that the aircraft can survive severe weather conditions. Given different LOC events (for example, a jammed actuator or stuck control surface), the existing LOC prevention methods focus on the computations of the safe set, especially in control constraints design of the flight control systems. However, it is difficult to anticipate all different adverse operating scenarios in the automatic control systems since the LOC occurs due to a combination of various factors, and detecting an impending LOC mode in real-time during an upset can be very challenging. In one study, up to 700 feet altitude loss occurred by linearized natural damping recovery for the aerodynamic envelopes. Such LOC recovery is more likely to experience a crash considering the terrain, especially during approach and landing. Such performance would not be considered an effective LOC recovery by the Pilot Guide to Airplane Upset Recovery, which requires that the altitude loss must be within 30m (100 feet).

[0010] Various control methods have been used striving to provide passengers with a smooth ride and high degree of safety. Order-reduction, decoupling, linearization and frozen time techniques are commonly used to develop the control system for LOC prevention and recovery. However, flight control systems are designed typically for nominal aircraft Equation-of-Motions (EOMs), which are invalid under upset conditions. In addition, such methods provide limited capabilities because the effectiveness or even stability of such designs relies heavily on the simplification assumptions pertaining to the specific LOC mode and aircraft models. In addition, perturbations caused by order-reduction (singular perturbation), decoupling (regular perturbation), linearization

(vanishing regular perturbation), and/or frozen time (non-vanishing regular perturbation) have typically been neglected during design relying on the stability margins to accommodate. In that case, the adequate stability margin and load/stress factors have not been given adequate attention in the controller design due to changes in the aircraft dynamics, possible excitation of un-modeled parasitic dynamics and parameter change by the upset. Furthermore, pilot LOC training requires the disengagement of autopilot when aircraft experiences upset, which clearly indicates the deficiencies and immaturity of the current automatic flight control systems in LOC recovery.

[0011] Therefore, significant improvements to the current LOC prevention and recovery performance by the existing techniques could be achieved with more advanced control techniques. There is a need for a more intelligent and reliable automatic LOC prevention and recovery system to supplement the pilot operation or even substitute for the pilot to control the aircraft in an upset condition.

Summary

[0012] An integrated loss-of-control prevention and recovery automatic control system of a fixed-wing aircraft is disclosed. The control system includes a plurality of flight control modes, including a nominal flight control mode, a loss-of-control prevention control mode, a loss-of-control arrest control mode, and a nominal flight restoration control mode. The control system further includes a supervisory control system capable of monitoring the flight states and flight events of the aircraft and determining which flight control mode to activate. In one aspect of the control system, the nominal flight control mode is defined by a six degree-of-freedom trajectory tracking controller with the wind-triangle and the post-stall aerodynamic characteristics in the calculation of the aerodynamic forces, and the time-varying parallel differential eigenvalues implemented in the feedback control gain matrices per Eqs. (9)-(11) below. In another aspect of the control system, the loss-of-control prevention control mode includes a bandwidth adaptation to the nominal flight control mode to prevent a loss of control of the aircraft. In another aspect of the control system the loss-of control prevention control mode employs time-varying parallel differential eigenvalues to sacrifice tracking performance to increase capability of tolerance for severe wind and other abnormalities in real-time. In yet another aspect of the control system, wherein the loss-of-control prevention control mode augments the six degree-of-freedom trajectory tracking controller in the nominal flight control mode via the gain matrices per Eqs. (9)-(11) below. In another

aspect of the control system, the loss-of-control arrest control mode includes a full throttle control during an arrest phase. In still another aspect of the control system, the loss-of-control arrest control mode includes a commanded aerodynamic attitude determined by a level and straight flight trim value of angle-of-attack and zero sideslip and bank angles. The loss-of-control arrest control mode may track the commanded aerodynamic profile via inner and outer aerodynamic attitude loops.

[0013] In another aspect of the control system, the restoration mode includes a close-in sub-mode for guiding the aircraft to catch up with a target position dictated by a mission trajectory and a home-in sub-mode for restoring the mission trajectory of the aircraft. The close-in sub-mode may be defined by a guidance approach wherein a velocity vector of the aircraft is aligned to a line-of-sight vector of the aircraft using proportional-integral-derivative linear regulation in an Earth reference frame. The home-in sub-mode may include a bandwidth adaptation for gradually regaining tracking performance of the aircraft and restoring the mission trajectory of the aircraft.

[0014] In another aspect of the control system, the supervisory control system includes a supervisory control logic variable having a value set according to flight states and flight events of the aircraft, and determining which flight control mode to activate. The supervisory control logic variable may be set to a value corresponding to the nominal flight control mode when a predetermined set of flight states of the aircraft are each within a predetermined set of operation thresholds. The supervisory control logic variable may be set to a value corresponding to the loss-of-control prevention control mode when at least one the flight states of the aircraft is within a predetermined set of protection thresholds. The supervisory control logic variable may be set to a value corresponding to the loss-of-control arrest control mode when at least one the flight states of the aircraft exceeds a predetermined set of safety thresholds. The supervisory control logic variable may be set to a value corresponding to the nominal flight restoration control mode when a predetermined set of flight states of the aircraft are each within a predetermined set of operation thresholds and a position error between the aircraft and a target position exceeds a range threshold.

[0015] A method of preventing loss-of-control of a fixed-wing aircraft having an automatic control system is also disclosed, The method includes monitoring a plurality of flight states of the aircraft, engaging a nominal flight control mode of the automatic control system when a predetermined set of flight states of the aircraft are each within a predetermined set of operation thresholds, engaging a prevention mode of the

automatic control system when at least one of the flight states of the aircraft is within a predetermined set of protection thresholds, and engaging a loss-of-control arrest mode of the automatic control system when at least one the flight states of the aircraft exceeds a predetermined set of safety thresholds. In one aspect of the method, it further includes engaging a restoration mode of the automatic control system when a predetermined set of flight states of the aircraft are each within a predetermined set of operation thresholds and a position error between the aircraft and a target position exceeds a range threshold.

[0016] In another embodiment, an integrated loss-of-control prevention and recovery automatic control system of a fixed-wing aircraft is also disclosed. The control system includes a plurality of flight control modes, including a nominal flight control mode and a loss-of-control prevention control mode. The control system also includes a supervisory control system capable of monitoring the flight states and flight events of the aircraft and determining which flight control mode to activate.

[0017] In another embodiment, an integrated loss-of-control prevention and recovery automatic control system of a fixed-wing aircraft is disclosed. The control system includes a plurality of flight control modes, including a nominal flight control mode and a loss-of-control arrest control mode. The control system further includes a supervisory control system capable of monitoring the flight states and flight events of the aircraft and determining which flight control mode to activate.

[0018] In another embodiment, a restoration mode for a fixed-wing aircraft is disclosed. The control system includes a close-in sub-mode for guiding the aircraft to catch up with a target position, wherein the close-in sub-mode is defined by a guidance approach wherein a velocity vector of the aircraft is aligned to a line-of-sight vector of the aircraft using proportional-integral-derivative linear regulation in an Earth reference frame. The control system further includes a home-in sub-mode for restoring a mission of the aircraft, wherein the home-in sub-mode includes a bandwidth adaptation for gradually regaining tracking performance of the aircraft and restoring the mission trajectory of the aircraft.

Brief Description of the Drawings

[0019] The accompanying drawings, which are incorporated in and constitute a part of this specification, illustrate embodiments of the invention and, together with a

general description of the invention given above, and the detailed description given below, serve to explain the invention.

[0020] Fig. 1 is a perspective view of an exemplary aircraft, further showing various coordinate frames relative to the aircraft.

[0021] Fig. 2A is a top view of the aircraft of Fig. 1, further showing a horizontal view of a wind triangle.

[0022] Fig. 2B is a top view similar to Fig. 2A, further showing a vertical view of a wind triangle.

[0023] Fig. 3 is a graph illustrating typical lift and drag coefficients varying with angle of attack for an exemplary aircraft.

[0024] Fig. 4 is a block diagram illustrating an exemplary loss-of-control prevention controller augmentation in accordance with an aspect of the invention.

[0025] Fig. 5 is a block diagram illustrating an adaptive gain structure in accordance with an aspect of the invention.

[0026] Fig. 6 is a graph illustrating bandwidth adaptation gain in accordance with an aspect of the invention.

[0027] Fig. 7 is a block diagram illustrating a loss-of-control arrest control mode configuration in accordance with an aspect of the invention.

[0028] Fig. 8 is a graph illustrating an exemplary wind condition in defining the severe wild tolerance capability.

[0029] Fig. 9 is a block diagram illustrating a multimodal control system configuration in accordance with an aspect of the invention.

[0030] Fig. 10 is a perspective view of an exemplary aircraft, further showing a line-of-sight vector and a velocity vector of the aircraft with respect to a mission trajectory of the aircraft.

[0031] Fig. 11 is a block diagram illustrating a steering control for a restoration mode in accordance with an aspect of the invention.

[0032] Fig. 12 is a block diagram illustrating a velocity control for a restoration mode in accordance with an aspect of the invention.

[0033] Fig. 13 is a graph illustrating a bandwidth adaptation law for a nominal mode, a close-in sub-mode, and a home-in sub-mode, in accordance with an aspect of the invention.

[0034] Fig. 14 is a block diagram of an autonomous flight management system that integrates the multimodal adaptive flight controller for Loss-of-Control Prevention and Recovery in accordance with an aspect of the invention.

[0035] Fig. 15 is a graph illustrating the definition of aircraft flight state threshold sets in accordance with an aspect of the invention.

[0036] Fig. 16 is a block diagram illustrating interrelationships between nominal, prevention, loss-of-control arrest, and restoration modes, and the mode transition logics, in accordance with an aspect of the invention.

Detailed Description

A. Nomenclature

[0037] The following is a list of the nomenclature used in the detailed description and drawings.

$\mathbf{P} = [x_e \quad y_e \quad z_e]^T$ = vehicle inertial position (m)

$\mathbf{V} = [u \quad v \quad w]^T$ = body frame vehicle velocity (m/s)

$\mathbf{A}_b = [a_u \quad a_v \quad a_w]^T$ = body frame acceleration (m/s^2)

$\mathbf{V}_a = [u_a \quad v_a \quad w_a]^T$ = body frame wind velocity (m/s)

$\mathbf{V}_t = [u_t \quad v_t \quad w_t]^T$ = body frame relative wind velocity (m/s)

$\mathbf{\Gamma} = [\phi \quad \theta \quad \psi]^T$ = Euler angles: roll, pitch, and yaw (rad)

$\mathbf{\Omega} = [p \quad q \quad r]^T$ = angular rates in the body frame (rad/s)

$\Theta = [a_p \quad a_q \quad a_r]^T$ = angular acceleration in the body frame (rad/s^2)

$\mathbf{\Delta} = [\delta_a \quad \delta_e \quad \delta_r]^T$ = aileron, elevator and rudder deflection (rad)

$\mathbf{F} = [F_x \quad F_y \quad F_z]^T$ = total force on aircraft in the body frame (N)

$\mathbf{F}_a = [D \quad Y \quad L]^T$ = aerodynamic force: drag, side force, and lift in the wind frame (N)

$\mathbf{T}_m = [L_m \quad M_m \quad N_m]^T$ = total torque on aircraft in the body frame (Nm)

$\mathbf{T} = [T_x \quad T_y \quad T_z]^T$ = body frame thrust (N)

$\mathbf{\Lambda} = [\alpha \quad \beta \quad \mu]^T$ = aerodynamic angles: angle-of-attack, sideslip and bank

	angle (rad)
$\mathbf{R}=[R_N \quad R_E \quad R_D]^T$	= range vector (m)
$\mathbf{LOS}=[l_1 \quad l_2 \quad l_3]^T$	= Line-of-Sight vector
$h=-z_e$	= altitude (m)
Q	= dynamic pressure (N/m^2)
$\bar{\rho}$	= local atmosphere density (kg/m^3)
V_t	= magnitude of vehicle velocity (m/s)
γ, χ	= flight path angle, heading angle (rad)
δ_T	= proportional thrust control effector
T, $T_{\max}$	= thrust magnitude, maximum thrust magnitude (N)
$V_{t,\max}$	= maximum allowable vehicle velocity (m/s)
W	= vehicle weight under conventional gravitational acceleration (N)
m	= vehicle mass (kg)
g	= gravitational acceleration (m/s^2)
S	= wing reference area (m^2)
b	= wing span (m)
$\bar{c}$	= wing mean aerodynamic chord (m)
n	= load factor
ρ	= azimuth angle (rad)
σ	= elevation angle (rad)
$\bar{r}$	= range vector magnitude
$flag$	= supervisory control flag
K_P, K_I, K_D	= proportional, integral and differential gain
K_V , K_r	= velocity and range regulation gains
α_{ij1}	= $\omega_n^2(t)$, where $\omega_n(t)$ is the time-varying natural frequency of desired dynamics for i^{th} loop, $i=1,2,3,4$, j^{th} channel, $i=1,2,3$, (1 = roll channel, 2 = pitch channel, 3 = yaw

	channel)
α_{ij2}	$=2\zeta\omega_n(t)$, where ζ is the constant damping ratio of desired dynamics for i^{th} loop, j^{th} channel
k_a	= bandwidth adaptation gain
$P(s)$	= plant transfer function
$L(s)$	= loop gain
$\phi(s)$	= phase response
ω_B	= actuator system bandwidth (rad/s)
ω_{cg}	= gain cross-over frequency of loop gain (rad/s)
ε	= singular perturbation parameter
ω_n	= natural frequency (rad/s)
$C_{D_0}, C_{D_\alpha}, C_{D_\beta}$	= drag force coefficients
C_{Y_β}, $C_{Y_{\delta r}}$	= side force coefficients
C_{L_0}, C_{L_α}, $C_{L_{\delta e}}$	= lift force coefficients
C_{l_β}, $C_{l_{\delta a}}$, $C_{l_{\delta r}}$	= roll moment coefficients
C_{m_o}, C_{m_α}, $C_{m_{\delta e}}$	= pitch moment coefficients
C_{n_β}, $C_{n_{\delta a}}$, $C_{n_{\delta r}}$	= yaw moment coefficients
I_{xx}, I_{yy}, I_{zz}	= moment of inertia about the body frame axis ($kg.m^2$)
I_{yz}, I_{xz}, I_{xy}	= products of inertia ($kg.m^2$)
$I^p_{pq}, I^q_{pp}, I^r_{pq}, I^p_{qr}, I^q_{pr}, I^r_{qr}$ $I^q_{rr}, g^p_l, g^p_n, g^r_l, g^q_m, g^r_n$	= inertia coefficients
I_x, I_y, I_z, I_{xz}	= moments of inertia
O_1, O_2, O_3	= operation box subset
P_1, P_2, P_3	= protection box subset
S_1, S_2, S_3	= safety box subset
S_x	= sin(x)
C_x	= cos(x)
T_x	= tan(x)

B. Reference Frames

[0038] The following aircraft coordinate frames are illustrated in Fig. 1.

[0039] The Earth-fixed reference frame F_E with flat-Earth assumptions is considered an inertial frame throughout this detailed description. A position vector in this frame is given as $P=\begin{bmatrix}x_E & y_E & z_E\end{bmatrix}^T$, with positive x_E pointing due north, y_E due east, and z_E toward the center of the Earth. The origin is some fixed point on the Earth's surface $P=\begin{bmatrix}0 & 0 & 0\end{bmatrix}$ that is specified when necessary.

[0040] A body-fixed frame of reference F_B is defined with the x-axis pointing forward along and parallel to the fuselage of the aircraft, and the y-axis at 90° along the right (starboard) wing such that the $x-z$ plane is the plane of symmetry of the aircraft. The z-axis points downward to form a right-handed triad. It is assumed that the thrust vector T runs along the x-axis and through the center-of-gravity (cg). A proportional thrust law given by $T_{\text{com}}=\delta_\tau T_{\max}$ is used for simplicity of exposition, where $\delta_\tau \in [0,1]$ denotes the engine throttle setting and is used as a control effector by the guidance control allocation.

[0041] The wind frame of reference F_W is defined with the x-axis along the total velocity vector V_t and the y-axis at 90° along the right (starboard) side of the aircraft aligned with the body frame y-axis. The z-axis remains at all times in the aircraft plane of symmetry, and completes a right-handed coordinate system.

[0042] A local atmospheric-fixed reference frame F_A describing the motion of the atmosphere with translational and rotational properties has its origin fixed in the air mass surrounding the aircraft and aligns with the Earth Frame when there is no rotational movement.

[0043] The equations of motion (EOM) are integrated in the body frame, and the aerodynamic forces and moments may be calculated in either the wind frame or body frame using appropriate aerodynamic coefficients. Using these reference frames leads to the standard EOM for a rigid-body aircraft.

[0044] There is also a body-carried Earth reference frame, sometimes called the "local Level Frame" or "local Geodetic Frame," which is to attach the origin of the Earth-fixed frame to the center of gravity of the aircraft without rotations. This frame may be useful in defining the aircraft attitude (orientation).

C. Introductory Overview

[0045] The invention provides an autonomous integrated Loss-of-Control Prevention and Recovery (iLOCPR) system capable of acting as a supervisory control to make decisions and coordinate various control modes according to the flight conditions of the aircraft. The iLOCPR system may be characterized by a set of one or more control modes including, for example, a "nominal flight control mode", a "LOC prevention control mode", a "LOC arrest control mode" and a "nominal flight restoration control mode." Generally, the functions of these modes are: (i) a baseline flight controller for 6DOF trajectory tracking as the nominal flight control mode designed by Trajectory Linearization Control (TLC); (ii) a bandwidth adaption augmentation to the baseline controller for LOC prevention control mode using the time-varying Parallel Derivative (PD)-eigenvalues to trade tracking performance for increased stability margin and robustness in the presence of LOC-prone flight conditions; (iii) a controller reconfiguration for LOC arrest control mode by switching from the trajectory tracking task to the aerodynamic angle tracking in order to recover and maintain healthy flight conditions at the cost of temporarily abandoning the mission trajectory; and (iv) a guidance trajectory designer for nominal flight restoration control mode after the successful arrest of a LOC upset. The iLOCPR system may also be used in manned aircraft for pilot assistance.

D. Nominal Flight Control Mode Design

[0046] The invention may include a nominal, or baseline, flight control mode. In one embodiment, the TLC 6DOF flight controller disclosed in U.S. Patent No. 8,761,966 ("the '966 patent"), the disclosure of which is incorporated by reference herein in its entirety, may be used.

1. Improved Bank-to-Turn in Guidance Control

[0047] It will be appreciated that in the TLC 6DOF flight controller, the Bank-to-Turn (BTT) guidance was not optimally designed for the tracking error feedback control of the side force control allocation, since the side force was allocated into commanded sideslip angle β_{com} so that the undesirable sideslip occurs. To minimize the undesired sideslip, a roll maneuver command defined by the *auxiliary roll* ϕ_{aux} may be introduced in this BTT improvement design. By rolling the aircraft, lateral component Y_{com} of the commanded lift L_{com} is used to provide the desired side force, thereby eliminating the undesired sideslip by

$$Y_{\text{com}} = L_{\text{com}} \sin\phi_{\text{aux}} \tag{1}$$

where we have assumed the body-frame roll angle equals to the aerodynamic bank angle μ under small angle-of-attack α and sideslip angle β . Thus, the auxiliary roll can be obtained as

$$\phi_{\text{aux}} = \arcsin\left(\frac{Y_{\text{com}}}{L_{\text{com}}}\right) \tag{2}$$

Therefore, the commanded roll angle is given by the following equation as

$$\phi'_{\text{com}} = \phi_{\text{com}} + \phi_{\text{aux}} \tag{3}$$

where ϕ_{com} is obtained from

$$\Gamma = \begin{bmatrix} \phi \\ \theta \\ \psi \end{bmatrix} = \begin{bmatrix} \tan^{-1}\left(\Upsilon \dfrac{C_\beta}{C_\alpha} \dfrac{\left(a-b^2\right)+b\tan\alpha\sqrt{c\left(1-b^2\right)+\Upsilon^2 S_\beta^2}}{a^2-b^2\left(1+c\tan^2\alpha\right)}\right) \\ \tan^{-1}\dfrac{ef+S_\gamma\sqrt{e^2-S_\gamma^2+f^2}}{e^2-S_\gamma^2} \\ \tan^{-1}\left\{\dfrac{\left(S_\mu S_\alpha - C_\alpha C_\mu S_\beta\right)C_\chi + \left[C_\gamma C_\alpha C_\beta - S_\gamma\left(S_\alpha C_\mu + S_\beta C_\alpha S_\mu\right)\right]S_\chi}{-\left(S_\mu S_\alpha - C_\alpha C_\mu S_\beta\right)S_\chi + \left[C_\gamma C_\alpha C_\beta - S_\gamma\left(S_\alpha C_\mu + S_\beta C_\alpha S_\mu\right)\right]C_\chi}\right\} \end{bmatrix} \tag{4}$$

2. Wind Effect on Navigation and Aerodynamics

[0048] Other improvements may be made to the TLC 6DOF flight controller. For example, since the weather factor plays a significant role in aircraft motion and aerodynamics, the wind effect needs to be considered. In order to describe the atmosphere properties and the airflow (wind) movement relative to the inertial frame, the local atmospheric-fixed reference frame representing the air-mass surrounding the aircraft is added as a body-carried frame with its origin fixed at the center-of-gravity of the aircraft.

[0049] The three-dimensional local wind inertial velocity $\mathbf{V}_a = \begin{bmatrix} u_a & v_a & w_a \end{bmatrix}^T$, the vehicle velocity $\mathbf{V} = [u \quad v \quad w]^T$ and the relative air velocity $\mathbf{V}_t = [u_t \quad v_t \quad w_t]^T$ can be expressed in the body frame as

$$\mathbf{V}_t = \mathbf{V} - \mathbf{V}_a = \begin{bmatrix} u_t \\ v_t \\ w_t \end{bmatrix} = \begin{bmatrix} u \\ v \\ w \end{bmatrix} - \begin{bmatrix} u_a \\ v_a \\ w_a \end{bmatrix} \tag{5}$$

This wind vectors relationship is called the wind triangle as depicted in Figs. 2A-2B. In addition to the heading angle χ and flight path angle γ describing the direction of the flight in the Inertial frame, the horizontal and vertical wind triangle components are defined as the crab angle $\chi_c = \chi - \psi$ and the air-mass-referenced flight-path angle $\gamma_a = \theta - \alpha$, respectively. These two wind-related angles are defined to navigate the vehicle in the inertial frame for trajectory tracking in the presence of wind. In this case, the commanded Euler attitude described in Eq. (4) is redesigned as follows when considering the wind triangle

$$\mathbf{\Gamma}_{\text{com}} = \begin{bmatrix} \phi_{\text{com}} \\ \gamma_a + \alpha \\ \chi - \chi_c \end{bmatrix} \tag{6}$$

where the wind triangle can be approximately calculated by

$$\gamma_a = \gamma + \arcsin\left(\frac{1}{V_t} \begin{bmatrix} w_n \\ w_e \\ w_d \end{bmatrix}^T \begin{bmatrix} \mathrm{C}_\chi \mathrm{S}_\gamma \\ \mathrm{S}_\chi \mathrm{S}_\gamma \\ \mathrm{C}_\gamma \end{bmatrix} \right), \quad \chi_c = \arcsin\left(\frac{1}{V_t \mathrm{C}_{\gamma_a}} \begin{bmatrix} w_n \\ w_e \end{bmatrix}^T \begin{bmatrix} -\mathrm{S}_\chi \\ \mathrm{C}_\chi \end{bmatrix} \right) \tag{7}$$

Note that the inertial wind velocity vector $\mathbf{V}_a = [u_a \quad v_a \quad w_a]^T$ is estimated by subtracting the sensed relative wind velocity $\mathbf{V}_{t,\text{sen}}$ from the sensed vehicle velocity $\mathbf{V}_{\text{sen}}$. It is emphasized that these changes only apply to the feedback error stabilizers, whereas the open-loop nominal controller is unaffected as the nominal wind velocity is assumed to be zero.

[0050] As a system parameter, the dynamic pressure depends on the local density of the atmosphere $\bar{\rho}$ and the airspeed V_t as $Q = \frac{1}{2}\bar{\rho}V_t^2$, which is implemented according to the relative wind velocity obtained by Eq. (5). Also, the aerodynamic angles are determined by the relative wind velocity as:

$$\alpha = \arctan\left(\frac{w_t}{u_t}\right),\ \beta = \arcsin\left(\frac{v_t}{V_t}\right),\ \mu = \arctan\left(\frac{u_t v_t \mathrm{S}_\theta + (u_t^2 + w_t^2)\mathrm{S}_\phi \mathrm{C}_\theta - u_t w_t \mathrm{C}_\phi \mathrm{C}_\theta}{V_t(w_t \mathrm{S}_\theta + u_t \mathrm{C}_\phi \mathrm{C}_\theta)}\right) \quad (8)$$

In implementation, V_t, $\bar{p}$, α, and β can be readily measured by an air data probe, and the ground speed can be obtained from satellite based GPS or ground-based navigation systems.

3. Stall Characteristics

[0051] For LOC arrest control, post-stall aerodynamic coefficients may be added to the TLC 6DOF flight controller in order to calculate the aerodynamic forces under stall conditions. Fig. 3 provides the aerodynamic lift and drag coefficients in full flight envelope for typical fixed-wing aircraft according to the wind-tunnel test results.

[0052] While the above improvements have been described with respect to the TLC 6DOF flight controller, they may be incorporated into any other suitable nominal or baseline design, as may be desired.

E. LOC Prevention Control Mode Design (Bandwidth Adaptation)

[0053] The baseline controller is capable of accommodating moderate wind conditions to maintain the inertial trajectory tracking task. Based on the singular perturbation theory, severe wind can be managed at the cost of reduced tracking performance by reducing the bandwidth (integral gain) of the closed-loop tracking error dynamics. The TLC 6DOF flight controller comprises four loops, and each loop has three channels, corresponding to the 6DOF in four loops. Accordingly, 12 second-order linear time-varying closed-loop tracking error dynamics

$$\ddot{x}_{ij} + \alpha_{ij2}(t)\dot{x}_{ij} + \alpha_{ij1}(t)x_{ij} = 0,\ i = 1,2,3,4,\ j = 1,2,3 \quad (9)$$

are synthesized using the constant damping time-varying PD-eigenvalues

$$\rho_{ij}(t) = \left(-\zeta_{ij} \pm j\sqrt{1-\zeta_{ij}^2}\right)\omega_{n,ij}(t),\ i = 1,2,3,4,\ j = 1,2,3 \quad (10)$$

by the PD-spectral synthesis formula

$$\alpha_{ij1}(t) = \omega_{n,ij}^2(t),\ \ \alpha_{ij2}(t) = 2\zeta_{ij}\omega_{n,ij}(t) - \frac{\dot{\omega}_{n,ij}(t)}{\omega_{n,ij}(t)},\ i = 1,2,3,4,\ j = 1,2,3 \quad (11)$$

where the index i is the loop number counting from outer loop to inner loop and j is the channel number; $\omega_{n,ij}(t)$ are time-varying natural frequencies and ζ_{ij} are the constant damping ratios of the desired closed-loop dynamics for each state variable x_{ij}.

However, constant natural frequencies $\omega_{n,ij}(t) \equiv \omega_{n,\text{nom}}$ were used for the baseline controller in the TLC 6DOF controller in the '966 patent, therefore, Eq. (11) was reduced to the familiar LTI synthesis formula, and the closed-loop dynamics were LTI in nature.

[0054] By way of example and without limitation, time-varying natural frequency $\omega_{n,ij}(t)$, which is proportional and approximately equal to the closed-loop (instantaneous) bandwidth, will be used herein for a real-time trade-off between tracking performance and robustness to prevent LOC. In this case, a TLC based adaptive control is proposed in Fig. 4, where the aircraft model is subject to wind disturbance and perturbation; and the control system is augmented with a time-varying bandwidth adaptive controller. Both the baseline controller and the adaptive controller rely on the feedback from the on-board navigation system.

1. The General Bandwidth Adaptation Law

[0055] For a multi-loop flight controller, wind effects that reduce the effective bandwidth of an inner-loop such as integrator windup can be treated as an increase in singular perturbation to its outer loops. Therefore, by the singular perturbation (time-scale separation) principle, the bandwidths of the outer loops should be reduced accordingly to preserve stability at the cost of reduced tracking performance. This bandwidth adaptation scheme can be readily realized with the time-varying bandwidth $\omega_{n,ij}(t)$ in Eq. (11). A single adaptation gain $k_a(t)$ will be used for all bandwidths

$$\omega_{n,ij}(t) = k_a(t)\omega_{n,ij,nom} \tag{12}$$

where the constant bandwidths $\omega_{n,ij,nom}$ are those of the nominal flight control mode as given in Table 1, which will be called nominal bandwidths. These values are exemplary only, and the $\omega_{n,ij,nom}$ should be designed for the specific aircraft. Thus, the $\omega_{n,ij,nom}$ are aircraft-dependent. The $\omega_{n,ij,nom}$ are first synthesized and tuned for the desired tracking performance with reasonable robustness in no wind condition. In addition, the $\zeta_{ij,nom}$ values shown in Table 1 are typical, and can be tuned for optimal performance. Based on the singular perturbation principle, Table 2 gives the expected behaviors of tracking performance and wind tolerance under bandwidth adaptation, where the Tolerable Wind Amplitude (TWA) can be used as a measure of the wind tolerance capability; $\|x_{error}\|_1$ is the cumulative state tracking error measured in L_1-norm; $k_{a,\min}$ and

$k_{a,\max}$ are the extreme values of $k_a(t)$ beyond which stability will be lost due to an exceedance of stability margins.

Table 1. Nominal TLC controller parameters.

	Loop 1			Loop 2			Loop 3			Loop 4		
	x	y	z	u	v	w	ϕ	θ	ψ	p	q	r
$\omega_{n,ij,nom}$	0.075	0.075	0.005	0.075	0.005	0.098	0.098	0.005	0.098	0.390	0.036	0.390
$\zeta_{ij,nom}$	1.414	1.414	1.414	1.414	1.414	1.414	1.414	1.414	1.414	1.414	1.414	1.414

Table 2. Bandwidth adaptation, expected TWA and tracking performance.

Adaptation Constant	**Bandwidth**	**TWA**	$\|x_{error}\|_1$
$k_{a,\min}$	$\omega_{n,\min}$	$V_{a,\max}$	$\|x_{error}\|_{1,\max}$
$k_{a,\text{nom}}$	$\omega_{n,\text{nom}}$	$V_{a,\text{nom}}$	$\|x_{error}\|_{1,\text{nom}}$
$k_{a,\max}$	$\omega_{n,\max}$	$V_{a,\min}$	$\|x_{error}\|_{1,\min}$

According to Eq. (12),

$$\frac{\dot{\omega}_{n,ij}(t)}{\omega_{n,ij}(t)} = \frac{\omega_{n,ij,nom}\dot{k}_a(t)}{\omega_{n,ij,nom}k_a(t)} = \frac{\dot{k}_a(t)}{k_a(t)} \tag{13}$$

Therefore, the PD-spectral synthesis formula in Eq. (11) can be rewritten as

$$\alpha_{ij1}(t) = \alpha_{ij1,\text{nom}}k_a^2(t),\ \alpha_{ij2}(t) = \alpha_{ij2,\text{nom}}k_a(t) - \frac{\dot{k}_a(t)}{k_a(t)}, \tag{14}$$

The bandwidth adaptation gain $k_a(t)$ and $\dot{k}_a(t)$ can be implemented using a first-order pseudo-differentiator as shown in Fig. 5, where ω_{LP} is a design parameter that determines the time constant of the $k_a(t)$ in response to a step command $k_{a,\text{desire}}(t)$. The time-varying coefficients $\alpha_{ij1}(t)$ and $\alpha_{ij2}(t)$ are then programmed into the baseline controller to replace the corresponding constant coefficients in the constant PI gain

matrices K_{P_i}, K_{I_i} described in the '966 patent.

2. Wind Adaptation Law Design

[0056] As shown in Table 3, with modifications as described above, the extreme bandwidths $\omega_{n,\min}$ and $\omega_{n,\max}$, TWA along with the corresponding tracking error metric are experimentally determined under each wind case. The numbers shown are presented for a particular aircraft and are intended to be exemplary only, and the amplitude of the wind in determining the TWA is defined using a standardized wind profile as shown in Fig. 8. It will be appreciated that the invention applies more broadly to any aircraft, including those having values different than those shown. Note that in Table 3, the tracking error metric $\|x_{\text{error}}\|_1$ goes up as k_a decrease and goes down as k_a increases, in support of the rationale for the bandwidth adaptation. Note also that the adaptation gain is reduced to 0.01 when downdraft is accommodated, which means the trajectory tracking is practically abandoned temporarily to prevent the vehicle from wind-induced LOC.

Table 3. Bandwidth adaptation, TWA and tracking error under wind conditions

Wind Condition	$\omega_{n,\min}$			$\omega_{n,\text{nom}}$			$\omega_{n,\max}$		
	$k_{a,\min}$	TWA	$\|x_{\text{error}}\|_1$	$k_{a,\text{nom}}$	TWA	$\|x_{\text{error}}\|_1$	$k_{a,\max}$	TWA	$\|x_{\text{error}}\|_1$
Tailwind	0.1	19	1.7e05	1	5	6.3e04	1.2	1	2.5e04
Headwind	0.1	80	434.4	1	75	1.2	1.2	15	0.3
Crosswind	0.1	25	6.1e04	1	7	3.2e04	1	4	3.2e03
Downdraft	0.01	25	9.9e04	1	3	2.9	1.2	2	0.9
Updraft	0.3	6	1.4e04	1	1	11.9	1.2	1	1.4

The adaptation laws are designed based on $\mathbf{V}_{a,\text{sen}} = \mathbf{V}_{\text{sen}} - \mathbf{V}_{t,\text{sen}}$, where the onboard ground speed sensor and airspeed sensor will be required to estimate the wind velocity. Then the time-varying bandwidth adaptation laws can be described on each wind case as in Table 4:

Table 4. Wind adaptation law.

Wind Condition	Adaptation Gain
Tailwind	$k_a(u_a,0,0) = \begin{cases} -0.06u_a + 1 & 0 \le u_a \le 15 \\ 0.1 & u_a > 15 \end{cases}$

Headwind	$k_a(u_a,0,0)=\begin{cases}1 & -75\le u_a\le 0\\ 0.1 & u_a<-75\end{cases}$
Crosswind	$k_a(0,v_a,0)=\begin{cases}-0.036v_a+1 & 0\le\lvert v_a\rvert\le 25\\ 0.1 & \lvert v_a\rvert>25\end{cases}$
Downdraft	$k_a(0,0,w_a)=\begin{cases}-0.33w_a+1 & 0<w_a\le 3\\ 0.01 & w_a>3\end{cases}$
Updraft	$k_a(0,0,w_a)=\begin{cases}0.3 & w_a<-1\\ 1 & -1\le w_a<0\end{cases}$

For wind velocity vector with three non-zero components acting in the body frame, the bandwidth adaptation law is designed by

$$\omega_n(t)=k_a(t)\omega_{n,\text{nom}},\ \text{where } k_a(t)=\min\left(k_a(u_a,0,0),k_a(0,v_a,0),k_a(0,0,w_a)\right) \tag{15}$$

where the k_a is inherited from the adaptation law design for individual wind case in Table 4. Such adaptation can ensure the minimum bandwidth requirement for longitudinal, vertical and lateral wind combination. Fig. 6 shows the adaptation gain k_a for the three-dimensional wind speed when $w_a=0\ m/s$. It will be appreciated that while the values shown in Table 4 are for a specific type of aircraft, these are intended to be exemplary only and the invention applies more broadly to other aircraft having different values.

F. LOC Arrest Control Mode Design

[0057] LOC Arrest Control Mode is designed to guarantee the aircraft to stay within a healthy aerodynamic envelope even at the cost of momentarily abandoning trajectory tracking objective. Once LOC is detected, a logic may be used to switch the controller automatically to LOC Arrest Control Mode from any of the control modes that the controller is in, where all other control modes use the baseline controller.

1. Switching Logic

[0058] In one embodiment, a switching flag is set to be active when LOC occurs; then the baseline flight controller needs to be disarmed. Such operation is achieved by setting tracking command equal to the sensed flight states including $\mathbf{P}_{\text{sen}}$, $\mathbf{V}_{\text{sen}}$, $\mathbf{\Gamma}_{\text{sen}}$, $\mathbf{\Omega}_{\text{sen}}$, so that the tracking errors are always zero. The integrations in the baseline controller for tracking control is disengaged. Meanwhile, the LOC Arrest Control Mode needs to be

engaged to take control of the aircraft.

2. Wind Frame EOM

[0059] The rotational kinematic EOM in the Wind Frame, rotational dynamics EOM in the Body-Fixed Frame are given as follows

Rotational Kinematics (Body Frame relative to Wind Frame)

$$\begin{bmatrix}\dot{\alpha}\\ \dot{\beta}\\ \dot{\mu}\end{bmatrix}=\begin{bmatrix}-\mathrm{T}_\beta \mathrm{C}_\alpha & 1 & -\mathrm{T}_\beta \mathrm{S}_\alpha\\ \mathrm{S}_\alpha & 0 & -\mathrm{C}_\alpha\\ \mathrm{C}_\alpha/\mathrm{C}_\beta & 0 & \mathrm{S}_\alpha/\mathrm{C}_\beta\end{bmatrix}\begin{bmatrix}p\\ q\\ r\end{bmatrix}+\begin{bmatrix}\Sigma_1\\ \Sigma_2\\ \Sigma_3\end{bmatrix}$$

$$\dot{\Lambda}=B_5(\Lambda)\Omega+f_5(\Lambda) \tag{16}$$

where $\Lambda=[\alpha \quad \beta \quad \mu]^T$ is the aerodynamic attitude vector and

$$\Sigma_1=-\frac{1}{mV\,\mathrm{C}_\beta}(L+T\,\mathrm{S}_\alpha)+\frac{g\,\mathrm{C}_\gamma \mathrm{C}_\mu}{V\,\mathrm{C}_\beta}$$

$$\Sigma_2=\frac{1}{mV}(D\,\mathrm{S}_\beta+Y\,\mathrm{C}_\beta-T\,\mathrm{C}_\alpha\,\mathrm{S}_\beta)+\frac{g\,\mathrm{C}_\gamma\,\mathrm{S}_\mu}{V}$$

$$\Sigma_3=\frac{1}{mV}[D\,\mathrm{T}_\gamma\,\mathrm{S}_\beta \mathrm{C}_\mu+Y\,\mathrm{T}_\gamma\,\mathrm{C}_\beta \mathrm{C}_\mu+L(\mathrm{T}_\beta+\mathrm{T}_\gamma\,\mathrm{S}_\mu)$$
$$+T(\mathrm{T}_\gamma\,\mathrm{S}_\alpha\,\mathrm{S}_\mu+\mathrm{S}_\alpha\,\mathrm{T}_\beta-\mathrm{T}_\gamma\,\mathrm{C}_\alpha\,\mathrm{S}_\beta \mathrm{C}_\mu)]-\frac{g\,\mathrm{C}_\gamma \mathrm{C}_\mu\,\mathrm{T}_\beta}{V}$$

in which D,Y,L are the aerodynamic force components drag, sideforce, and lift, respectively.

Rotational Dynamics

$$\begin{bmatrix}\dot{p}\\ \dot{q}\\ \dot{r}\end{bmatrix}=\begin{bmatrix}g_l^p & 0 & g_n^p\\ 0 & g_m^q & 0\\ g_l^r & 0 & g_n^r\end{bmatrix}\begin{bmatrix}L_m\\ M_m\\ N_m\end{bmatrix}+\begin{bmatrix}I_{pq}^p pq+I_{pr}^p qr\\ I_{pp}^q p^2+I_{rr}^q r^2+I_{pr}^q pr\\ I_{pq}^r pq+I_{qr}^r qr\end{bmatrix} \tag{17}$$

$$\dot{\boldsymbol{\Omega}}=B_6\mathbf{T}_\mathrm{m}+f_6(\boldsymbol{\Omega})$$

where ??=$[p \quad q \quad r]^T$ is the angular velocity vector. The LOC Arrest Control Mode TLC control configuration is illustrated in Fig. 7.

3. LOC Arrest Control Mode Command

[0060] The commanded aerodynamic attitude $\Lambda_{\mathrm{arst}}=[\alpha_{\mathrm{arst}} \quad \beta_{\mathrm{arst}} \quad \mu_{\mathrm{arst}}]^T=[\alpha_{\mathrm{trim}} \quad 0 \quad 0]^T$ can be determined by the level and straight flight trim value of angle-of-attack as $W=L=\bar{Q}S\left(C_{L_0}+C_{L_\alpha}\alpha_{\mathrm{trim}}\right)$ and zero sideslip and bank angles, where the dynamic pressure $\bar{Q}$ is chosen by desired value of the end of the arrest based on the altitude and airspeed.

On the other hand, a level flight path angle $\gamma'_{com} = 0^\circ$ is commanded depending on allowable altitude loss. In order to quickly recover the healthy aerodynamic attitude, the full throttle control $\delta_{T,arst} = 1$ is applied. This full throttle effect for arrest operation would require a "mission restoration" controller (discussed below) to be designed at the end of the arrest to restore the throttle command and to redirect the aircraft back to the mission trajectory.

4. Aerodynamic Attitude Outer Loop

[0061] In an exemplary embodiment, the controller is designed to track the commanded aerodynamic profile using TLC and the controller configuration, as shown in Fig. 7.

[0062] The outer loop of the aerodynamic attitude control takes in aerodynamic attitude command $\Lambda_{nom} = \Lambda_{com}$ and the sensed states Λ_{sen} to calculate the body rate command for the inner loop. For aerodynamic attitude tracking, the nominal body rate is given by inverting (16)

$$\Omega_{nom,2} = B_5^{-1}(\Lambda_{nom})(\dot{\Lambda}_{nom} - f_5(\Lambda_{nom})) \tag{18}$$

Then with the tracking error $\Lambda_{err} = \Lambda_{sen} - \Lambda_{com}$, the Proportional-Integral (PI) feedback control law is obtained from the desired PD-eigenvalues based TLC design as shown below.

$$\Omega_{ctrl,2} = -K_{P5}(t)\Lambda_{err} - K_{15}(t)\int\Lambda_{err} \tag{19}$$

where

$$K_{P5} = \begin{bmatrix} k_{p5,11} & k_{p5,12} & k_{p5,13} \\ k_{p5,21} & k_{p5,22} & k_{p5,23} \\ k_{p5,31} & k_{p5,32} & k_{p5,33} \end{bmatrix}, K_{15} = \begin{bmatrix} 0 & \alpha_{521}S_\alpha & \alpha_{531}C_\alpha C_\beta \\ \alpha_{511} & 0 & \alpha_{531}S_\beta \\ 0 & -\alpha_{512}C_\alpha & \alpha_{531}S_\alpha C_\beta \end{bmatrix} \tag{20}$$

in which

$$
\begin{aligned}
k_{p5,11} &= \frac{T}{mV}(C_\alpha^2 C_\beta S_\mu T_\gamma + S_\alpha C_\alpha S_\beta C_\beta C_\mu T_\gamma + S_\beta) + r \\
k_{p5,12} &= S_\alpha\left[\alpha_{322} + \frac{1}{mV}(DC_\beta - YS_\beta - TC_\alpha C_\beta)\right] \\
&\quad + \frac{1}{mVC_\beta}[C_\alpha(L + TS_\alpha - mgC_\mu C_\gamma + DC_\beta^3 C_\mu T_\gamma \\
&\quad - TC_\alpha C_\beta^3 C_\mu T_\gamma - YS_\beta C_\beta^2 C_\mu T_\gamma)] + pC_\alpha^2 T_\beta + rS_\alpha C_\alpha T_\beta \\
k_{p5,13} &= \frac{1}{mV}[C_\alpha C_\beta(\alpha_{332} mV + LC_\mu T_\gamma + TS_\alpha C_\mu T_\gamma - DS_\beta S_\mu T_\gamma \\
&\quad + YC_\beta S_\mu T_\gamma + WT_\beta S_\mu C_\gamma + TC_\alpha S_\beta S_\mu T_\gamma) - WS_\alpha S_\mu C_\gamma] \\
k_{p5,21} &= \frac{1}{mV}[-TS_\alpha C_\beta^2 C_\mu T_\gamma - TC_\alpha C_\beta + TS_\alpha C_\mu T_\gamma \\
&\quad + TC_\alpha S_\beta S_\mu T_\gamma] + \alpha_{312} \\
k_{p5,22} &= \frac{T_\gamma}{mV}[-YC_\mu + YC_\beta^2 C_\mu + DS_\alpha C_\beta C_\mu \\
&\quad - TC_\alpha S_\beta C_\beta C_\mu] - pC_\alpha - rS_\alpha \\
k_{p5,23} &= \frac{1}{mV}[S_\beta(LC_\mu T_\gamma + TS_\alpha C_\mu T_\gamma - DS_\beta S_\mu T_\gamma - YC_\beta S_\mu T_\gamma \\
&\quad + mgT_\beta S_\mu C_\gamma + TC_\alpha S_\beta S_\mu T_\gamma) - mgS_\mu C_\gamma / C_\beta] + \alpha_{332} S_\beta \\
k_{p5,31} &= \frac{TT_\gamma}{mV}(S_\alpha C_\alpha C_\beta S_\mu - S_\alpha^2 S_\beta C_\beta C_\mu) - p \\
k_{p5,32} &= \frac{1}{mVC_\beta}[S_\alpha(L + TS_\beta - mgC_\mu C_\gamma + DC_\beta^3 C_\mu T_\gamma \\
&\quad - TC_\alpha C_\beta^3 C_\mu T_\gamma - YS_\beta C_\beta^2 C_\mu T_\gamma)] + pS_\alpha C_\alpha T_\beta \\
&\quad + rS_\alpha^2 T_\beta - C_\alpha[\alpha_{322} - \frac{1}{mV}(YS_\beta - DC_\beta + TC_\alpha C_\beta)] \\
k_{p5,33} &= \frac{1}{mV}[S_\alpha C_\beta(LC_\mu T_\gamma + TS_\alpha C_\mu T_\gamma - DS_\beta S_\mu T_\gamma \\
&\quad - YC_\beta S_\mu T_\gamma + mgT_\beta S_\mu C_\gamma + TC_\alpha S_\beta S_\mu T_\gamma) \\
&\quad + mgC_\alpha S_\mu C_\gamma] + \alpha_{332} S_\alpha C_\beta
\end{aligned}
\tag{21}
$$

The gain matrices are synthesized from the time-varying PD-eigenvalues by the desired closed-loop behavior of the tracking error dynamics. The output of the attitude outer-loop controller is then obtained as

$$
\boldsymbol{\Omega}_{\text{com},2} = \boldsymbol{\Omega}_{\text{nom},2} + \boldsymbol{\Omega}_{\text{ctrl},2} \tag{22}
$$

5. Aerodynamic Attitude Inner Loop

[0063] The nominal moment vector is calculated by inverting (17) to obtain $\mathbf{T}_{m,\text{nom},2} = B_6^{-1}\left[\dot{\boldsymbol{\Omega}}_{\text{nom},2} - f_6\left(\boldsymbol{\Omega}_{\text{nom},2}\right)\right]$, and the PI control law for this loop is

$$\mathbf{T}_{m,\mathrm{ctrl},2} = -\mathbf{K}_{\mathrm{P6}}\boldsymbol{\Omega}_{\mathrm{err},2} - \mathbf{K}_{16}\int_{t_0}^{t}\boldsymbol{\Omega}_{\mathrm{err},2}(\sigma)d\sigma \tag{23}$$

where $\boldsymbol{\Omega}_{\mathrm{err},2} = \boldsymbol{\Omega}_{\mathrm{sen}} - \boldsymbol{\Omega}_{\mathrm{com},2}$ and

$$\mathbf{K}_{\mathrm{P4}} = \begin{bmatrix} I_{xx}\left(\alpha_{412} + I^{p}_{pq}\bar{q}\right) - I^{r}_{pq}I_{xz}\bar{q} \\ I_{yy}\left(2I^{q}_{pp}\bar{p} + I^{q}_{pr}\bar{r}\right) \\ -I_{xz}\left(I^{p}_{pq}\bar{q} + \alpha_{412}\right) + I_{zz}I^{r}_{pq}\bar{q} \end{bmatrix}$$

$$\begin{bmatrix} I_{xx}\left(I^{p}_{pq}\bar{p} + I^{p}_{pr}\bar{r}\right) - I_{xz}\left(I^{r}_{pq}\bar{p} + I^{r}_{qr}\bar{r}\right) & I_{xx}I^{p}_{qr}\bar{q} - I_{xz}\left(I^{r}_{qr}\bar{q} + \alpha_{432}\right) \\ \alpha_{422}I_{yy} & I_{yy}\left(2I^{q}_{rr}\bar{r} + I^{q}_{pr}\bar{p}\right) \\ -I_{xz}\left(I^{p}_{pq}\bar{p} + I^{p}_{qr}\bar{r}\right) + I_{zz}\left(I^{r}_{pq}\bar{p} + I^{r}_{qr}\bar{r}\right) & -I_{xz}I^{p}_{qr}\bar{q} + I_{zz}\left(I^{r}_{qr}\bar{q} + \alpha_{432}\right) \end{bmatrix}$$

$$\mathbf{K}_{\mathrm{I4}} = \begin{bmatrix} I_{xx}\alpha_{411} & 0 & -I_{xz}\alpha_{431} \\ 0 & I_{yy}\alpha_{421} & 0 \\ -I_{xz}\alpha_{411} & 0 & I_{zz}\alpha_{431} \end{bmatrix}$$

The commanded moment is then given by

$$\mathbf{T}_{m,\mathrm{com},2} = \mathbf{T}_{m,\mathrm{nom},2} + \mathbf{T}_{m,\mathrm{ctrl},2} \tag{24}$$

6. Attitude Control Allocation

[0064] The moment equations are written in terms of the control effectiveness Jacobian, so that

$$\begin{bmatrix} L_m - QSbC_{l_\beta}\beta \\ M_m - QS\bar{c}(C_{m_0} + C_{m_\alpha}\alpha) \\ N_m - QSbC_{n_\beta}\beta \end{bmatrix} = \begin{bmatrix} QSbC_{l_{\delta a}} & 0 & QSbC_{l_{\delta_r}} \\ 0 & QS\bar{c}C_{m_{\delta_e}} & 0 \\ QSbC_{n_{\delta a}} & 0 & QSbC_{n_{\delta_r}} \end{bmatrix} \begin{bmatrix} \delta_a \\ \delta_e \\ \delta_r \end{bmatrix} \tag{25}$$

and inversion of (25) gives the control surface deflections command as:

$$\boldsymbol{\Delta}_{\mathrm{arst}} = \begin{bmatrix} QSbC_{l_{\delta a}} & 0 & QSbC_{l_{\delta_r}} \\ 0 & QS\bar{c}C_{m_{\delta_e}} & 0 \\ QSbC_{n_{\delta a}} & 0 & QSbC_{n_{\delta_r}} \end{bmatrix}^{-1} \begin{bmatrix} L_{m,\mathrm{com}} - QSbC_{l_\beta}\beta_{\mathrm{com}} \\ M_{m,\mathrm{com}} - QS\bar{c}\left(C_{m_0} + C_{m_\alpha}\alpha_{\mathrm{com}}\right) \\ N_{m,\mathrm{com}} - QSbC_{n_\beta}\beta_{\mathrm{com}} \end{bmatrix} \tag{26}$$

G. Nominal Flight Restoration Control Mode Design

[0065] The position tracking errors may increase to beyond the capability of the nominal flight control mode after the LOC arrest. A nominal flight restoration control mode may therefore be needed in order to reduce the position tracking error to a level that can be accommodated by the nominal flight control mode to eventually restore the mission.

1. Nominal Flight Restoration Control Mode Configuration

[0066] The nominal flight restoration control mode configuration in the multi-modal control system iLOCPR is shown in Fig. 9, in which the mission trajectory is

replaced by a restoration trajectory as the command trajectory in order to direct the vehicle back to the mission trajectory after a successful arrest of upset.

[0067] Assuming a virtual aircraft that is moving along the mission trajectory at a prescribed time, such virtual target can be referred as a target point, whose position is predefined in the inertial frame. At the end of LOC arrest, the flight envelope determining healthy flight states is recovered as

$$\Lambda \in O_1 \text{ AND } \Omega \in O_2 \text{ AND } V_t \in O_3 \tag{27}$$

where

$$\begin{aligned} O_1 &= \left\{\Lambda : \alpha \in [-2^\circ, 5^\circ],\ \beta \in [-5^\circ, 5^\circ],\ \mu = \left[-20^\circ, 20^\circ\right]\right\} \\ O_2 &= \left\{\Omega : p,q,r \in [-20^\circ/\sec, 20^\circ/\sec]\right\} \\ O_3 &= \left\{V_t \in [1.5V_{\text{stall}}, V_{\max}]\right\} \end{aligned} \tag{28}$$

where $\Lambda = [\alpha \quad \beta \quad \mu]^T$ are the aerodyanmic angles; $\Omega = [p \quad q \quad r]^T$ are the angular rates; V_{stall} and $V_{\max}$ are the vehicle stall speed and the maximum achievable speed, respectively. The values given in Eq. (28) are exemplary only, and other values may be used depending on the particular aircraft. Flight envelope O_1, O_2, O_3 indicates the success of the LOC arrest. At this moment, the nominal flight restoration control mode is engaged by setting the supervisory control *flag* = 3 as shown in Table 5. Under this controller mode, the command trajectory is switched to $\mathbf{P}_{\text{com}} = \mathbf{P}_{\text{rstr}}$; the feedback variables are the same as the ones designed for the nominal flight control mode as $\mathbf{P}_{\text{sen}}$, $\mathbf{V}_{\text{sen}}$, Γ_{sen}, Ω_{sen}; and the controller outputs are Δ_{com}, $\delta_{\text{r,com}}$.

Table 5. Multi-Mode Controller Configuration

Mode	*flag*	Trajectory	Active Controller	Controller Output
Nominal	0	$\mathbf{P}_{\text{tgt}}$	6DOF Nominal	Δ_{com}, $\delta_{\text{r,com}}$
Prevention	1	$\mathbf{P}_{\text{tgt}}$	6DOF Nominal + BW Adaptation	Δ_{com}, $\delta_{\text{r,com}}$
Arrest	2	Λ_{arst}	3DOF Arrest	Δ_{arst}, $\delta_{\text{r,arst}}$
Restoration	3	$\mathbf{P}_{\text{rstr}}$	6DOF Nominal	Δ_{com}, $\delta_{\text{r,com}}$

[0068] By sensing the current position $\mathbf{P}_{sen}$ and reading the target point $\mathbf{P}_{tgt}$ at each sampling time, the range vector, which represents the position tracking error, can be obtained in real-time as

$$\begin{aligned}\mathbf{R} &= [R_N \quad R_E \quad R_D]^T \\ &= \mathbf{P}_{tgt} - \mathbf{P}_{sen} = [x_{tgt} \quad y_{tgt} \quad z_{tgt}]^T - [x_{sen} \quad y_{sen} \quad z_{sen}]^T\end{aligned} \tag{29}$$

where the range vector $\mathbf{R}$ is described in NED Cartesian coordinate. However, the position tracking error is normally very large, since the altitude loss and course deviations usually occur during the LOC arrest.

[0069] In order to restore the original mission, two sequential sub-modes are designed for the mission restoration mode. The first sub-mode is called "close-in," in which a restoration trajectory $\mathbf{P}_{rstr}$ is planned to reduce the range given in (29) to a moderate level, which will be defined as a capture box. Once the range is in the capture box, a sub-mode called "home-in" is designed to gradually restore the original mission. The design of these two sub-modes will be described as follows.

2. Close-in Control

[0070] The pure pursuic guidance (PPG) strategy is employed to cope with the large range vector (29) in the Cartesian coordinate by transforming it to the spherical coordinate as follows

$$\begin{aligned}\rho &= \arctan\left(\frac{R_E}{R_N}\right) \\ \sigma &= -\arcsin\left(\frac{R_D}{r}\right) \\ r &= \sqrt{R_N^{\,2} + R_E^{\,2} + R_D^{\,2}}\end{aligned} \tag{30}$$

where r is the range vector magnitude; ρ is the azimuth angle and σ is the elevation angle, respectively. Therefore, the range vector $\mathbf{R} = [R_N \quad R_E \quad R_D]^T$ can be determined by the azimuth angle and the elevation angle as follows

$$\begin{aligned}R_N &= r\cos\rho\cos\sigma \\ R_E &= r\sin\rho\cos\sigma \\ R_D &= -r\sin\sigma\end{aligned} \tag{31}$$

As shown in (31), the components ρ and σ indicate the orientation in the inertial frame. Such orientation is called the LOS vector, which is defined as $\mathbf{LOS} = [l_1 \quad l_2 \quad l_3]^T$ whose three components are shown as below

$$\begin{aligned} l_1 &= \cos\rho\cos\sigma \\ l_2 &= \sin\rho\cos\sigma \\ l_3 &= -\sin\sigma \end{aligned} \tag{32}$$

where l_1 , l_2 and l_3 are the three-dimensional normalized coordinates in the NED Cartesian frame. As shown in Fig. 10, the LOS vector is determined by the azimuth angle and the elevation angle of the range vector described in (30), but with the normalized magnitude. On the other hand, the aircraft inertial velocity vector $\mathbf{v} = [\dot{x} \quad \dot{y} \quad \dot{z}]^T$ is represented using the flight course components as

$$\begin{aligned} \dot{x} &= V\cos\chi\cos\gamma \\ \dot{y} &= V\sin\chi\cos\gamma \\ \dot{z} &= -V\sin\gamma \end{aligned} \tag{33}$$

where the χ is the heading angle and γ is the flight-path angle, respectively; V is the inertial vehicle velocity magnitude. Fig. 10 also shows the vehicle velocity vector and its flight-path components in the inertial frame.

[0071] The PPG trajectory design is to align the vehicle velocity vector with the LOS by steering and accelerating the vehicle. The Restoration Trajectory block in Fig. 9 can be expanded as shown in Fig. 11, in which the first two channels are used for orientation regulation, and the third channel is dedicated to velocity control according to the distance and the target velocity, which are described below.

[0072] With respect to orientation control, as shown in Fig. 10, the vehicle's velocity vector is regulated to point to the target direction indicated by LOS in (33). Therefore, the azimuth and elevation angles ρ and σ that determine the LOS vector in (31) and (32) are employed as the guidance commands for the close-in orientation design

$$\chi_{\text{gui}} = \rho,\ \gamma_{\text{gui}} = \sigma \tag{34}$$

and the following PID control laws are designed as:

$$\begin{aligned} \chi_{\text{rstr}} &= K_{p_\chi}\chi_{\text{err}} + K_{I_\chi}\int_0^t \chi_{\text{err}}(\tau)d\tau + K_{D_\chi}\dot{\chi}_{\text{err}} \\ \gamma_{\text{rstr}} &= K_{p_\gamma}\gamma_{\text{err}} + K_{I_\gamma}\int_0^t \gamma_{\text{err}}(\tau)d\tau + K_{D_\gamma}\dot{\gamma}_{\text{err}} \end{aligned} \tag{35}$$

where $\chi_{\text{err}} = \chi_{\text{gui}} - \chi_{\text{sen}}$ and $\gamma_{\text{err}} = \gamma_{\text{gui}} - \gamma_{\text{sen}}$ are the feedback tracking errors for the heading angle channel and the flight-path angle channel, respectively, which are both

assumed to be sufficiently small, which is satisfied with the vehicle behind the target with a large range and relatively small altitude and horizontal course deviation; χ_{sen} and γ_{sen} are the sensed vehicle heading angle and flight-path angle, respectively; and the χ_{rstr} and γ_{rstr} are the feedback control variables for the *close-in* trajectory generation.

[0073] With respect to velocity control, the velocity command comprises two sources: the distance r and the inertial speed of the virtual target V_{tgt}. At the end of the restoration, the vehicle velocity should be the same as the target speed V_{tgt}. Regarding the initial value setting for the integrators in the controller, at the nominal flight restoration control mode triggering moment when $t = t_r$, which is also the end of the arrest, even though the position command is set to $\mathbf{P}_{com} = \mathbf{P}_{rstr}$, the internal states of the controller are not consistent with those induced by $\mathbf{P}_{rstr}$. Therefore, the velocity vector of the restoration guidance trajectory $\mathbf{P}_{rstr}$ is initialized at $V_{sen}(t_r)$ to guide the velocity for 5s, as shown in Eq. (36). This phase is called *coast*, which effectively avoids the throttle saturation induced by excessive controller transient.

$$V_{ref} = \begin{cases} V_{sen}, & t_{rstr} \le t \le t_{rstr} + 5 \\ V_{tgt}, & t > t_{rstr} \end{cases} \tag{36}$$

After the controller is initialized, vector $\mathbf{v}_{tgt}$ is employed to guide the vehicle by the pure pursuit guidance law, which allows the Line-of-Sight (LOS) tracking to converge first while maintaining a constant range. Once the LOS errors $|y_e|$ and $|z_e|$ are sufficiently reduced to within a threshold δ, where δ is determined by the maximum thrust of the aircraft, the guidance velocity V_{ref} is increased for the vehicle to close-in onto the target based on the range by

$$V_r = \begin{cases} \text{sat}(r-1)k_r, & |y_e| < \delta \,\&\, |z_e| < \delta \\ 0, & \text{Otherwise} \end{cases} \tag{37}$$

where the saturation function on the range is set to, for instance, $2\,m/s$ depending on the maximum thrust of the aircraft, which limits the maximum increase in velocity due to the range error. It will be appreciated that this is an exemplary value only and may be different depending on the particular aircraft. The range induced acceleration is applied only when the range is larger than 1m. Therefore, the guidance velocity decreases to $V_{ref} = V_{tgt}$ as the range is reduced to less than 1m in preparation for home-in. Accordingly,

the guidance velocity control considering the mode switching mechanism is given as follows

$$\dot{V}_{\text{rstr}} = K_V \left(V_{\text{ref}} + V_r - V_{\text{rstr}} \right) \tag{38}$$

Then the Velocity Control block in Fig. 11 can be expanded as follows for the principle illustration and implementation as shown in Fig. 12. By the orientation χ_{rstr} and γ_{rstr}, and the velocity control V_{rstr} designs above, the guidance trajectory for mission restoration can be obtained by integrating the following inertial velocity in Cartesian coordinate as

$$\begin{aligned} \dot{x}_{\text{rstr}} &= V_{t,\text{rstr}} \cos\chi_{\text{rstr}} \cos\gamma_{\text{rstr}} \\ \dot{y}_{\text{rstr}} &= V_{t,\text{rstr}} \sin\chi_{\text{rstr}} \cos\gamma_{\text{rstr}} \\ \dot{z}_{\text{rstr}} &= V_{t,\text{rstr}} \sin\gamma_{\text{rstr}} \end{aligned} \tag{39}$$

The restoration trajectory $\mathbf{P}_{\text{rstr}} = [x_{\text{rstr}} \quad y_{\text{rstr}} \quad z_{\text{rstr}}]^T$ in (39) is then planned for the nominal controller to track. When the position tracking error between the vehicle and the target converges to within the boundaries indicated by the capture range box defined in (40), the close-in control is finished.

$$N = \left\{ \mathbf{R} : R_N \in [-1,1],\ R_E \in [-1,1],\ R_D = [-1,1] \right\} \tag{40}$$

It will be appreciated that the values shown in Eq. (40) are exemplary only and that other values may be used depending on the particular aircraft.

3. Home-in Control

[0074] After (40) is satisfied, the multi-modal controller is configured by switching the *flag* from value 3 to 0 as shown in Table 5 and Fig. 9, such configuration indicating that the mission trajectory $\mathbf{P}_{\text{tgt}}$ is restored. This section presents the second phase of mission restoration called home-in, which is designed for restoring the mission trajectory tracking precision.

[0075] At the end of the close-in sub-mode, there is still an amount of tracking error which is beyond the capability of the nominal tracking precision indicated by $\omega_{n,ij,\text{nom}}$, which is provided by desired tracking performance and reasonable system robustness. In this case, the robustness of the system needs to be increased to guarantee the system stability in order to accommodate the existing tracking error, then gradually restore the desired tracking performance. In order to trade off between the tracking

performance and the system robustness, the single-parameter adaptation law described for the LOC prevention control mode is employed for the home-in sub-mode

$$\omega_{n,ij}(t) = k_a(t)\omega_{n,ij,\text{nom}}, \quad i = 1,2,3,4, \; j = 1,2,3 \tag{41}$$

[0076] Based on the bandwidth adaptation philosophy shown in Fig. 13, a bandwidth adaptation law is implemented to the nominal controller according to (41) for a smooth transition to the nominal configuration. As shown in Fig. 13, the system bandwidth of the 6DOF nominal controller is adapted by $k_{a,\text{rstr}}(t)$, which is a moderate value in $(0,1)$ to ensure an adequate robustness and tracking performance for the close-in sub-mode. Such bandwidth adaptation gain is also the initial value for time-varying home-in gain $k_{a,\text{homein}}(t_0) = k_{a,\text{rstr}}(t)$, where t_0 indicates the moment that the system configuration switches to the home-in sub-mode. During the home-in sub-mode, the adaptation gain increases gradually in order to increase the tracking performance. Once $k_{a,\text{homein}}(t)$ is increased to the value 1 at t_1, the nominal mission is restored completely. The system under the application of its tuned-up bandwidth for the trajectory tracking mission.

H. Automatic Flight Management System (AFMS)

[0077] As previously mentioned, in one embodiment the invention provides an Autonomous Flight Management System (AFMS). An exemplary AFMS scheme is shown in Fig. 14. The AFMS may act as a supervisory control system which is capable of decision making and coordination of the different control modes according to the flight conditions of the aircraft. In other words, the supervisory control system is capable of monitoring the flight states and flight events of the aircraft and determining which flight control mode to activate or implement. The iLOCPR system is characterized by a set of one or more of the aforementioned control modes under the supervisory control of the AFMS.

[0078] Designed on the top level, the supervisory control AFMS has the switching logic variable "flag" as one of its output, whose value is set according to the real-time flight states and flight events. Each of the control modes corresponds to one flag value in the hybrid system finite state machine and can be transitioned automatically from one to another under specific conditions. Another output of the AFMS is the bandwidth adaptation gain, which is designed for the bandwidth augmentation under the specific control objectives for each mode. The bandwidth adaptation scheme is designed based

on the PD-eigenvalue theory, where the bandwidth of the multiple-nested-loop system can be adapted to make the tradeoff between the tracking performance and the system robustness.

[0079] The design of the AFMS finite-state machine entails specifying on the threshold boxes for the flight mode determination as illustrated in Fig. 15 and the state transition predicates shown in Fig. 16 and Table 6.

1. Quantification

[0080] Since an upset is the direct consequence of aerodynamic attitude exceedance of the normal flight envelope, the aerodynamic attitude is essential as a LOC indicator. In addition, angular rates also constitute a LOC indicator, as they must be kept within a certain range to prevent the wings and control surfaces from unbalanced stall induced by abnormal airflow. Another indicator is the airspeed, as stall will occur below the critical airspeed. Therefore, the vehicle safety can be described by three sets of thresholds, which consist of the extremities of aerodynamic attitude, angular rates, and airspeed as shown in Fig. 15. The "operation box" is defined by the thresholds as

$$\begin{aligned} O_1 &= \left\{\Lambda : \alpha \in [-2^\circ, 5^\circ],\ \beta \in [-5^\circ, 5^\circ],\ \mu = \left[-20^\circ, 20^\circ\right]\right\} \\ O_2 &= \left\{\Omega : p, q, r \in [-20\,\text{deg/sec}, 20\,\text{deg/sec}]\right\} \\ O_3 &= \left\{V_t \in [1.5V_{t,\text{stall}}, V_{t,\max}]\right\} \end{aligned} \tag{42}$$

where $\Lambda = [\alpha \quad \beta \quad \mu]^T$ are the aerodynamic angles, i.e. angle-of-attack, sideslip and bank angle respectively; $\Omega = [p \quad q \quad r]^T$ are the body-axis roll, pitch, yaw rotational rate; and V_t is the airspeed. The values shown in Eq. (42) are exemplary only and may be different depending on the particular aircraft. The operation box bounds the healthy flight state variables under the nominal mode. The "protection box" defines a buffer (hysteresis) zone between the nominal and LOC arrest mode up to the maximum allowable flight conditions as shown in Eq. (43) as

$$\begin{aligned} P_1 &= \left\{\begin{array}{l} \Lambda : \alpha \in 0.6\times[-5^\circ, 15^\circ],\ \beta \in 0.6\times[-10^\circ, 10^\circ], \\ \mu = 0.6\times\left[-45^\circ, 45^\circ\right] \end{array}\right\} \\ P_2 &= \left\{\Omega : p, q, r \in 0.6\times[-60\,\text{deg/sec}, 60\,\text{deg/sec}]\right\} \\ P_3 &= \left\{V_t \in 0.6\times[V_{t,\text{stall}}, V_{t,\max}]\right\} \end{aligned} \tag{43}$$

The values shown in Eq. (43) are exemplary only and may be different depending on the particular aircraft. The "safety box" is defined by the extremities of aerodynamic

angles, angular rates and airspeed given in Eq. (44) such that LOC will be declared when any one of them is exceeded.

$$\begin{aligned} S_1 &= \left\{\Lambda : \alpha \in [-5^\circ, 15^\circ],\ \beta \in [-10^\circ, 10^\circ],\ \mu = \left[-45^\circ, 45^\circ\right]\right\} \\ S_2 &= \{\Omega : p, q, r \in [-60\,\text{deg/sec}, 60\,\text{deg/sec}]\} \\ S_3 &= \left\{V_t \in [V_{t,\text{stall}}, V_{t,\max}]\right\} \end{aligned} \tag{44}$$

It is noted that the specific values of aerodynamic angles, angular rates, and airspeed used in Eq. (42-44) to define the flight conditions are exemplified here based on typical wind-tunnel flight data and LOC studies. In addition, a small range (position error between the target and the vehicle) box for the home-in sub-mode and a large range box for the restoration mode are defined respectively

$$\begin{aligned} R_{\text{small}} &= \{\mathbf{R} : \sqrt{R_N^2 + R_E^2 + R_D^2} \le 1\} \\ R_{\text{med}} &= \{\mathbf{R} : 1 < \sqrt{R_N^2 + R_E^2 + R_D^2} \le 50\} \\ R_{\text{large}} &= \{\mathbf{R} : \sqrt{R_N^2 + R_E^2 + R_D^2} > 50\} \end{aligned} \tag{45}$$

In practice, these threshold boxes should be defined on a case-by-case basis for the specific aircraft model and Fig. 15 simply provides a visual representation using 3D boxes. The supervisory control logic variable is then determined by

$$flag = \begin{cases} 0, & \Lambda \in O_1 \text{ AND } \Omega \in O_2 \text{ AND } V_t \in O_3 \text{AND } range \in R_{\text{small}} \\ 1, & \Lambda \in P_1 \setminus O_1 \text{ AND } \Omega \in P_2 \setminus O_1 \text{ AND } V_t \in P_3 \setminus O_3 \\ 2, & \Lambda \notin S_1 \text{ OR } \Omega \notin S_2 \text{ OR } V_t \notin S_3 \\ 3, & \text{AND } \Lambda \in O_1 \text{ AND } \Omega \in O_2 \text{ AND } V_t \in O_3 \text{ AND } range \in R_{\text{large}} \end{cases} \tag{46}$$

in which the $flag = 0$ value is set as long as the operation box defined in Eq. (42) is satisfied. The corresponding state for $flag = 0$ is the nominal flight control mode. If any flight condition exceeds the operation box, while all of the indicating flight conditions still stay in the protection box defined in Eq. (43), $flag = 1$, and the LOC prevention control mode is engaged. If any of the flight conditions exceeds the safety box defined in Eq. (44), $flag = 2$, which indicates the engagement of the LOC arrest control mode. When all the flight conditions return to inside of the operation box in Eq. (42) and large position error R_{large} occurs by Eq. (45), $flag = 3$ is set for the engagement of the nominal flight restoration control mode. When the R_{small} is recovered and all the flight states are within the operation box, the nominal flight control mode is reset with $flag = 0$.

2. Mode Transition

[0081] The AFMS is designed as a Moore finite-state machine. The interrelationships among each discrete mode are captured in the state transition diagram in Fig. 16.

Table 6. Transition and Condition for Finite-State Machine.

Transition	Condition
a	Exceed the protection box.
b	Inside the operation box, small range error.
c	Inside the safety box, large range error.
d	Exceed the safety box.
e	Inside the operation box, large range error.
f	Exceed the safety box.
g	Inside the operation box, small range error.

Transition a: Nominal→ Prevention

The nominal flight control mode (flag = 0) is the default mode when the system is initialized. The LOC prevention control mode (flag = 1) will not be turned on until the operation box is exceeded, while all states are inside the protection box, in which case the transition a is made and the LOC prevention control mode is enabled.

Transition b: Prevention → Nominal

By applying the LOC prevention control mode, if the operation box is recovered and the range loss (position tracking error) is small, the transition is triggered to enable the nominal flight control mode.

Transition c: Prevention → Restoration

If the prevention process causes a large range loss, the transition c is triggered to enable the nominal flight restoration control mode.

Transition d: Prevention → Arrest

LOC is declared when the safety box is exceeded. Moreover, at that time, the transition d is triggered to engage the LOC arrest control mode (flag = 2).

Transition e: Arrest → Restoration

On the other hand, when the operation box is successfully recovered by the LOC arrest control mode with a large range error, the transition e is made to trigger the nominal flight restoration control mode (flag = 3).

Transition f: Restoration → Arrest

During the nominal flight restoration control mode, if the safety box is exceeded again, the LOC arrest control mode is triggered by the transition f.

Transition g: Restoration → Nominal

After recovering the operation box, and range loss (position tracking error) is reduced by the nominal flight restoration control mode to within the R_{small} given in Eq. (45), the transition g is made. The nominal flight control mode is restored.

3. Multi-Modal Controller Integration

[0082] The multi-modal controller diagram is shown in Fig. 9. The nominal flight control mode is designed to execute the mission trajectory-tracking task. The LOC prevention control mode is designed by a bandwidth adaptation augmentation to the nominal flight control mode to trade off tracking performance with increased stability margin and robustness in the presence of LOC-prone flight conditions. In other words, tracking performance is sacrificed in order to increase the capability of tolerance for severe wind and other abnormalities in real time. The LOC arrest control mode is designed to switch from the mission trajectory-tracking task to aerodynamic attitude trajectory tracking task for LOC arrest in order to recover and maintain healthy flight condition at the cost of temporarily abandoning the mission trajectory. In the nominal flight restoration control mode, a guidance trajectory $\mathbf{P}_{rstr}$ is generated to direct the vehicle back to the mission trajectory after the successful arrest of a LOC upset and then restore the tracking performance.

[0083] Fig. 14 shows the multi-modal controller configuration under the AFMS including the supervisory control $flag$ value for configuring each control mode, the bandwidth adaptation gain k_a designed for each control mode, and Fig. 9 shows the corresponding command trajectory, controller, feedback variables, and controller outputs. The system configuration can also be described as shown in Table 7.

Table 7. Multi-Modal Controller Configuration.

Mode	Nominal	Prevention	Arrest	Restoration
flag	0	1	2	3
k_a	1	$k_{a,\text{prev}}$	$k_{a,\text{arst}}$	$k_{a,\text{rstr}}$
Trajectory	$\mathbf{P}_{\text{tgt}}$	$\mathbf{P}_{\text{tgt}}$	$\mathbf{\Lambda}_{\text{arst}}$	$\mathbf{P}_{\text{rstr}}$
Controller	Baseline	Baseline	Arrest	Baseline
Feedback Variable	$\mathbf{P}_{\text{sen}}, \mathbf{V}_{\text{sen}}, \mathbf{\Gamma}_{\text{sen}}, \mathbf{\Omega}_{\text{sen}}$	$\mathbf{P}_{\text{sen}}, \mathbf{V}_{\text{sen}}, \mathbf{\Gamma}_{\text{sen}}, \mathbf{\Omega}_{\text{sen}}$	$\mathbf{\Lambda}_{\text{sen}}, \mathbf{\Omega}_{\text{sen}}$	$\mathbf{P}_{\text{sen}}, \mathbf{V}_{\text{sen}}, \mathbf{\Gamma}_{\text{sen}}, \mathbf{\Omega}_{\text{sen}}$
Controller Output	$\mathbf{\Delta}_{\text{com}}, \delta_{r,\text{com}}$	$\mathbf{\Delta}_{\text{com}}, \delta_{r,\text{com}}$	$\mathbf{\Delta}_{\text{arst}}, \delta_{r,\text{arst}}$	$\mathbf{\Delta}_{\text{com}}, \delta_{r,\text{com}}$

4. Nominal Flight Control Mode Configuration

[0084] As shown in Table 7, the baseline TLC 6DOF controller is engaged to achieve the mission trajectory tracking goal.

[0085] Regarding the supervisory control, the nominal flight control mode corresponds to the supervisory control $flag = 0$ and $k_a = 1$. The nominal flight control mode aims to achieve the desired tracking performance with the tuned nominal bandwidth parameters without the bandwidth adaptation.

[0086] With respect to baseline controller engagement, when the baseline controller is engaged, the mission trajectory is selected to be the control objective under nominal flight control mode by applying $\mathbf{P}_{\text{com}} = \mathbf{P}_{\text{tgt}}$. The feedback states $\mathbf{P}_{\text{sen}}, \mathbf{V}_{\text{sen}}, \mathbf{\Gamma}_{\text{sen}}, \mathbf{\Omega}_{\text{sen}}$ are utilized to calculate the feedback stabilizing TLC gain matrices in real time. And the corresponding command trajectories for the baseline controller are configured as

$$\begin{aligned} \mathbf{V}_{\text{com}} &= \mathbf{V}_{\text{nom}} + \mathbf{V}_{\text{ctrl}}, & \mathbf{\Gamma}_{\text{com}} &= \mathbf{\Gamma}_{\text{nom}} + \mathbf{\Gamma}_{\text{ctrl}} \\ \mathbf{\Omega}_{\text{com1}} &= \mathbf{\Omega}_{\text{nom1}} + \mathbf{\Omega}_{\text{ctrl1}}, & \mathbf{T}_{m,\text{com1}} &= \mathbf{T}_{m,\text{nom1}} + \mathbf{T}_{m,\text{ctrl1}} \end{aligned} \tag{47}$$

where the command variables are obtained by adding the closed-loop PI feedback tracking error control with subscript "ctrl" to the nominal control with subscript "nom" from dynamic pseudo-inversion. In this case, the controller outputs $\left[\mathbf{\Delta}_{\text{com}},\ \delta_{r,\text{com}}\right]$ are selected.

[0087] With respect to LOC arrest control mode disengagement, meanwhile, the LOC arrest control mode is on standby by setting the aerodynamic attitude tracking command and the ensuing body rate command equal to the sensed flight states as

$$\mathbf{\Lambda}_{\text{com}} = \mathbf{\Lambda}_{\text{sen}},\ \mathbf{\Omega}_{\text{com2}} = \mathbf{\Omega}_{\text{sen}} \tag{48}$$

so that the integrators in the LOC arrest control mode are put on hold by setting zero tracking errors as $\mathbf{\Lambda}_{\text{err}} = \mathbf{\Lambda}_{\text{sen}} - \mathbf{\Lambda}_{\text{com}} = 0,\ \mathbf{\Omega}_{\text{err}2} = \mathbf{\Omega}_{\text{sen}} - \mathbf{\Omega}_{\text{com}2} = 0$.

[0088] Regarding the initial value setting for the integrators in the controller, the default controller mode is the nominal flight control mode. The initial values of the integrators of the baseline controller $\mathbf{P}_{\text{ini}}, \mathbf{V}_{\text{ini}}, \mathbf{\Gamma}_{\text{ini}}, \mathbf{\Omega}_{\text{ini}1}$ and the LOC arrest control mode $\mathbf{\Lambda}_{\text{ini}}, \mathbf{\Omega}_{\text{ini}2}$ are obtained by a trim flight condition.

5. LOC Prevention Control Mode Configuration

[0089] As shown in Table 7, the baseline controller is also employed for LOC prevention control mode.

[0090] Regarding the supervisory control, the LOC prevention control mode is in accordance with the supervisory control law as $flag = 1$. The LOC prevention adaptation law $k(t)_{a,\text{prev}}$ is applied to the baseline controller in order to a tradeoff between the tracking performance and the system robustness.

[0091] With respect to baseline controller engagement, the baseline controller is engaged. The mission trajectory, feedback states, command variables for each loop, and the controller outputs are set to be the same as the ones for the nominal flight control mode.

[0092] With respect to LOC arrest control mode disengagement, the LOC arrest control mode remains on standby by Eq. (48).

[0093] Regarding the initial value setting for the integrators in the multi-modal controller, in the LOC prevention control mode, all the state values for the integrators are inherited from the nominal flight control mode. Integrators of the LOC arrest control mode are storing the feedback states from the sensing system in preparation for a LOC.

6. LOC Arrest Control Mode Configuration

[0094] The baseline controller is disengaged for LOC arrest control mode, while the LOC arrest control mode is armed.

[0095] Regarding the supervisory control, once LOC is detected, the supervisory control is set as $flag = 2$. The bandwidth adaptation $k(t)_{a,\text{arst}}$ is applied for different LOC conditions.

[0096] With respect to baseline controller disengagement, the nominal flight control mode is disarmed by the following setting

$$\mathbf{P}_{\text{com}} = \mathbf{P}_{\text{sen}},\ \mathbf{V}_{\text{com}} = \mathbf{V}_{\text{sen}},\ \mathbf{\Gamma}_{\text{com}} = \mathbf{\Gamma}_{\text{sen}},\ \mathbf{\Omega}_{\text{com}1} = \mathbf{\Omega}_{\text{sen}} \tag{49}$$

which implies that all the integrators in the nominal control feedback loop are frozen by taking in zero tracking errors, since

$$\begin{aligned} &\mathbf{P}_{\text{err}} = \mathbf{P}_{\text{sen}} - \mathbf{P}_{\text{com}} = 0,\ \mathbf{V}_{\text{err}} = \mathbf{V}_{\text{sen}} - \mathbf{V}_{\text{com}} = 0, \\ &\boldsymbol{\Gamma}_{\text{err}} = \boldsymbol{\Gamma}_{\text{sen}} - \boldsymbol{\Gamma}_{\text{com}} = 0,\ \boldsymbol{\Omega}_{\text{err}1} = \boldsymbol{\Omega}_{\text{sen}} - \boldsymbol{\Omega}_{\text{com}1} = 0 \end{aligned} \tag{50}$$

[0097] With respect to LOC arrest control mode engagement, the LOC arrest control mode is taking control of the system, in which $\boldsymbol{\Lambda}_{\text{arst}}$ is the command for arresting the LOC.

$$\boldsymbol{\Lambda}_{\text{com}} = \boldsymbol{\Lambda}_{\text{arst}},\ \boldsymbol{\Omega}_{\text{com}2} = \boldsymbol{\Omega}_{\text{nom}2} + \boldsymbol{\Omega}_{\text{ctrl}2} \tag{51}$$

The control outputs $\left[\boldsymbol{\Delta}_{\text{arst}},\ \delta_{r,\text{arst}}\right]$ are selected.

[0098] Regarding the initial value setting for the integrators in the controller, the LOC arrest control mode is properly initialized by the sensed states of $\boldsymbol{\Lambda}_{\text{sen}}$ and $\boldsymbol{\Omega}_{\text{sen}}$ at the switching time so that switching transient or instability caused by excessive inertial tracking error is avoided.

7. Nominal Flight Restoration Control Mode Configuration

[0099] The baseline controller is engaged for nominal flight restoration control mode.

[00100] Regarding the supervisory control, the nominal flight restoration control mode corresponds to the supervisory control $flag = 3$. The bandwidth adaptation gain $k_{a,\text{rstr}}(t)$ is applied to increase the tracking error tolerance capability.

[00101] With respect to baseline controller engagement, the baseline controller is engaged. The mission trajectory is set to $\mathbf{P}_{\text{com}} = \mathbf{P}_{\text{rstr}}$. Otherwise, all feedback states, command variables for each loop and the controller outputs are set to be the same as the ones for the nominal mode design.

[00102] With respect to LOC arrest control mode disengagement, the arrest controller is disarmed by satisfying the Eq. (48).

[00103] Regarding the initial value setting for the integrators in the controller, at the restoration mode triggering moment when $t = t_r$, which is also the end of the arrest, even though the position command is set to $\mathbf{P}_{\text{com}} = \mathbf{P}_{\text{rstr}}$, the internal states of the controller are not consistent with those induced by $\mathbf{P}_{\text{rstr}}$. Therefore, the velocity vector of the restoration guidance trajectory $\mathbf{P}_{\text{rstr}}$ is initialized at $V_{\text{sen}}(t_r)$ to guide the velocity for 5s, as shown in Eq. (36). This phase is called *coast*, which effectively avoids the throttle saturation induced by excessive controller transient.

8. State Equation and Controller State

[00104] Additional details of designing the multi-modal controller shown as in Fig. 9 can be found in the '966 patent in accordance with the value of the supervisory signal flag.

[00105] Also, the state equations for the controller and the vehicle equation-of-motions are summarized in Tables 8-10, in which the coefficient matrices of the pseudo-differentiator is given as

$$\mathrm{A}_{\mathrm{diff},i} = \begin{bmatrix} \mathrm{O}_3 & \mathrm{I}_3 \\ \mathrm{A}_{21,i} & \mathrm{A}_{22,i} \end{bmatrix}, \mathrm{B}_{\mathrm{diff},i} = \begin{bmatrix} \mathrm{O}_3 \\ -\mathrm{A}_{21,i} \end{bmatrix}, i = 1,2,3,4,5,6$$

$$\mathrm{A}_{21,i} = \mathrm{diag}\left[-\omega_{n,\mathrm{diff},ij}^2 \quad -\omega_{n,\mathrm{diff},ij}^2 \quad -\omega_{n,\mathrm{diff},ij}^2\right] \tag{52}$$

$$\mathrm{A}_{22,i} = \mathrm{diag}\left[-2\zeta_{\mathrm{diff},ij}\omega_{n,\mathrm{diff},ij} \quad -2\zeta_{\mathrm{diff},ij}\omega_{n,\mathrm{diff},ij} \quad -2\zeta_{\mathrm{diff},ij}\omega_{n,\mathrm{diff},ij}\right]$$

where *i* represents the loop number, and *j* represents the channel number.

Table 8. Baseline Controller State Equations.

$\mathbf{P}_{\mathrm{com}}$	$\mathbf{P}_{\mathrm{nom}} = \mathbf{P}_{\mathrm{com}}$
$\mathbf{P}_{\mathrm{nom}}$, $\dot{\mathbf{P}}_{\mathrm{nom}}$	$\begin{bmatrix} \mathbf{P}_{\mathrm{nom}} \\ \ddot{\mathbf{P}}_{\mathrm{nom}} \end{bmatrix} = \mathbf{A}_{\mathrm{diff},1} \begin{bmatrix} \mathbf{P}_{\mathrm{nom}} \\ \dot{\mathbf{P}}_{\mathrm{nom}} \end{bmatrix} + \mathbf{B}_{\mathrm{diff},1} \mathbf{P}_{\mathrm{com}}$
GON	$\mathbf{V}_{\mathrm{nom}} = B_1^{-1}(\boldsymbol{\Gamma}_{\mathrm{nom}})\dot{\mathbf{P}}_{\mathrm{nom}}$
$\mathbf{P}_{\mathrm{err}}$	$\mathbf{P}_{\mathrm{err}} = \mathbf{P}_{\mathrm{sen}} - \mathbf{P}_{\mathrm{com}}$
GOF	$\mathbf{V}_{\mathrm{ctrl}} = -\mathbf{K}_{\mathrm{P1}}\mathbf{P}_{\mathrm{err}} - \mathbf{K}_{\mathrm{I1}}\int_0^t \mathbf{P}_{\mathrm{err}}(\tau)d\tau$
$\mathbf{V}_{\mathrm{com}}$	$\mathbf{V}_{\mathrm{com}} = \mathbf{V}_{\mathrm{nom}} + \mathbf{V}_{\mathrm{ctrl}}$
$\mathbf{V}_{\mathrm{nom}}$, $\dot{\mathbf{V}}_{\mathrm{nom}}$	$\begin{bmatrix} \dot{\mathbf{V}}_{\mathrm{nom}} \\ \ddot{\mathbf{V}}_{\mathrm{nom}} \end{bmatrix} = \mathbf{A}_{\mathrm{diff},2} \begin{bmatrix} \mathbf{V}_{\mathrm{nom}} \\ \dot{\mathbf{V}}_{\mathrm{nom}} \end{bmatrix} + \mathbf{B}_{\mathrm{diff},2} \mathbf{V}_{\mathrm{nom}}$
GIN	$\mathbf{F}_{\mathrm{nom}} = m\left[\dot{\mathbf{V}}_{\mathrm{nom}} - B_2(\boldsymbol{\Omega}_{\mathrm{nom}})\mathbf{V}_{\mathrm{nom}}\right]$
$\mathbf{V}_{\mathrm{err}}$	$\mathbf{V}_{\mathrm{err}} = \mathbf{V}_{\mathrm{sen}} - \mathbf{V}_{\mathrm{com}}$
GIF	$\mathbf{F}_{\mathrm{ctrl}} = -\mathbf{K}_{\mathrm{P2}}\mathbf{V}_{\mathrm{err}} - \mathbf{K}_{\mathrm{I2}}\int_0^t \mathbf{V}_{\mathrm{err}}(\tau)d\tau$
GAN	$\boldsymbol{\Gamma}_{\mathrm{nom}} = f_2(\mathbf{F}_{\mathrm{nom}})$
GAC	$\boldsymbol{\Gamma}_{\mathrm{com}} = f_2(\mathbf{F}_{\mathrm{com}})$
$\boldsymbol{\Gamma}_{\mathrm{nom}}$, $\dot{\boldsymbol{\Gamma}}_{\mathrm{nom}}$	$\begin{bmatrix} \dot{\boldsymbol{\Gamma}}_{\mathrm{nom}} \\ \ddot{\boldsymbol{\Gamma}}_{\mathrm{nom}} \end{bmatrix} = \mathbf{A}_{\mathrm{diff},3} \begin{bmatrix} \boldsymbol{\Gamma}_{\mathrm{nom}} \\ \dot{\boldsymbol{\Gamma}}_{\mathrm{nom}} \end{bmatrix} + \mathbf{B}_{\mathrm{diff},3} \boldsymbol{\Gamma}_{\mathrm{nom}}$
EON	$\boldsymbol{\Omega}_{\mathrm{nom}} = B_3^{-1}(\boldsymbol{\Gamma}_{\mathrm{nom}})\dot{\boldsymbol{\Gamma}}_{\mathrm{nom}}$
$\boldsymbol{\Gamma}_{\mathrm{err}}$	$\boldsymbol{\Gamma}_{\mathrm{err}} = \boldsymbol{\Gamma}_{\mathrm{sen}} - \boldsymbol{\Gamma}_{\mathrm{com}}$
EOF	$\boldsymbol{\Omega}_{\mathrm{ctrl}} = -\mathbf{K}_{\mathrm{P3}}\boldsymbol{\Gamma}_{\mathrm{err}} - \mathbf{K}_{\mathrm{I3}}\int_0^t \boldsymbol{\Gamma}_{\mathrm{err}}(\tau)d\tau$
$\boldsymbol{\Omega}_{\mathrm{com}1}$	$\boldsymbol{\Omega}_{\mathrm{com}1} = \boldsymbol{\Omega}_{\mathrm{nom}1} + \boldsymbol{\Omega}_{\mathrm{ctrl}1}$

$\boldsymbol{\Omega}_{\text{nom}1}$, $\dot{\boldsymbol{\Omega}}_{\text{nom}1}$	$\begin{bmatrix}\dot{\boldsymbol{\Omega}}_{\text{nom}1}\\ \ddot{\boldsymbol{\Omega}}_{\text{nom}1}\end{bmatrix}=\mathbf{A}_{\text{diff},4}\begin{bmatrix}\boldsymbol{\Omega}_{\text{nom}1}\\ \dot{\boldsymbol{\Omega}}_{\text{nom}1}\end{bmatrix}+\mathbf{B}_{\text{diff},4}\boldsymbol{\Omega}_{\text{nom}1}$
EIN	$\mathbf{T}_{m,\text{nom}1}=B_4^{-1}\left[\dot{\boldsymbol{\Omega}}_{\text{nom}1}-f_4\left(\boldsymbol{\Omega}_{\text{nom}1}\right)\right]$
$\boldsymbol{\Omega}_{\text{err}1}$	$\boldsymbol{\Omega}_{\text{err}1}=\boldsymbol{\Omega}_{\text{sen}}-\boldsymbol{\Omega}_{\text{com}1}$
EIF	$\mathbf{T}_{m,\text{ctrl}1}=-\mathbf{K}_{\text{P4}}\boldsymbol{\Omega}_{\text{err}1}-\mathbf{K}_{\text{I4}}\int_{t_0}^{t}\boldsymbol{\Omega}_{\text{err}1}(\sigma)d\sigma$
$\mathbf{T}_{m,\text{com}1}$	$\mathbf{T}_{m,\text{com}1}=\mathbf{T}_{m,\text{nom}1}+\mathbf{T}_{m,\text{ctrl}1}$
EA	$\boldsymbol{\Delta}_{\text{com}}=J^{-1}\mathbf{T}_{\text{allo}1}$

Table 9. LOC Arrest Control Mode State Equations.

$\boldsymbol{\Lambda}_{\text{rstr}}$	$\boldsymbol{\Lambda}_{\text{nom}}=\boldsymbol{\Lambda}_{\text{rstr}}$
$\boldsymbol{\Lambda}_{\text{nom}}$, $\dot{\boldsymbol{\Lambda}}_{\text{nom}}$	$\begin{bmatrix}\dot{\boldsymbol{\Lambda}}_{\text{nom}}\\ \ddot{\boldsymbol{\Lambda}}_{\text{nom}}\end{bmatrix}=\mathbf{A}_{\text{diff},5}\begin{bmatrix}\boldsymbol{\Lambda}_{\text{nom}}\\ \dot{\boldsymbol{\Lambda}}_{\text{nom}}\end{bmatrix}+\mathbf{B}_{\text{diff},5}\boldsymbol{\Lambda}_{\text{rstr}}$
$\boldsymbol{\Lambda}_{\text{err}}$	$\boldsymbol{\Lambda}_{\text{err}}=\boldsymbol{\Lambda}_{\text{sen}}-\boldsymbol{\Lambda}_{\text{rstr}}$
AOF	$\boldsymbol{\Omega}_{\text{ctrl}2}=-\mathbf{K}_{\text{P6}}\boldsymbol{\Lambda}_{\text{err}}-\mathbf{K}_{\text{I6}}\int_{t_0}^{t}\boldsymbol{\Lambda}_{\text{err}}(\tau)d\tau$
$\boldsymbol{\Omega}_{\text{com}2}$	$\boldsymbol{\Omega}_{\text{com}2}=\boldsymbol{\Omega}_{\text{nom}2}+\boldsymbol{\Omega}_{\text{ctrl}2}$
$\boldsymbol{\Omega}_{\text{nom}2}$, $\dot{\boldsymbol{\Omega}}_{\text{nom}2}$	$\begin{bmatrix}\dot{\boldsymbol{\Omega}}_{\text{nom}2}\\ \ddot{\boldsymbol{\Omega}}_{\text{nom}2}\end{bmatrix}=\mathbf{A}_{\text{diff},6}\begin{bmatrix}\boldsymbol{\Omega}_{\text{nom}2}\\ \dot{\boldsymbol{\Omega}}_{\text{nom}2}\end{bmatrix}+\mathbf{B}_{\text{diff},6}\boldsymbol{\Omega}_{\text{nom}2}$
AIN	$\mathbf{T}_{m,\text{nom}2}=B_4^{-1}\left[\dot{\boldsymbol{\Omega}}_{\text{nom}2}-f_4\left(\boldsymbol{\Omega}_{\text{nom}2}\right)\right]$
$\boldsymbol{\Omega}_{\text{err}2}$	$\boldsymbol{\Omega}_{\text{err}2}=\boldsymbol{\Omega}_{\text{sen}}-\boldsymbol{\Omega}_{\text{com}2}$
AIF	$\mathbf{T}_{m,\text{ctrl}2}=-\mathbf{K}_{\text{P4}}\boldsymbol{\Omega}_{\text{err}2}-\mathbf{K}_{\text{I4}}\int_{t_0}^{t}\boldsymbol{\Omega}_{\text{err}2}(\sigma)d\sigma$
$\mathbf{T}_{m,\text{com}2}$	$\mathbf{T}_{m,\text{com}2}=\mathbf{T}_{m,\text{nom}2}+\mathbf{T}_{m,\text{ctrl}2}$
AA	$\boldsymbol{\Delta}_{\text{arst}}=J^{-1}\mathbf{T}_{\text{allo}2}$

Table 10. Nominal Flight Restoration Control Mode State Equations.

$\mathbf{P}_{\text{err}}$ Spherical coordinate	$\rho=\arctan\left(\frac{R_E}{R_N}\right)$ $\sigma=-\arcsin\left(\frac{R_D}{r}\right)$ $r=\sqrt{R_N{}^2+R_E{}^2+R_D{}^2}$
γ_{err} , $\dot{\gamma}_{\text{err}}$	$\begin{bmatrix}\dot{\gamma}_{\text{err}}\\ \ddot{\gamma}_{\text{err}}\end{bmatrix}=\begin{bmatrix}0 & 1\\ -\omega_{n,\gamma}^2 & -2\zeta_\gamma\end{bmatrix}\begin{bmatrix}\gamma_{\text{err}}\\ \dot{\gamma}_{\text{err}}\end{bmatrix}+\begin{bmatrix}0\\ \omega_{n,\gamma}^2\end{bmatrix}\gamma_{\text{err}}$
χ_{err} , $\dot{\chi}_{\text{err}}$	$\begin{bmatrix}\dot{\chi}_{\text{err}}\\ \ddot{\chi}_{\text{err}}\end{bmatrix}=\begin{bmatrix}0 & 1\\ -\omega_{n,\chi}^2 & -2\zeta_\chi\end{bmatrix}\begin{bmatrix}\chi_{\text{err}}\\ \dot{\chi}_{\text{err}}\end{bmatrix}+\begin{bmatrix}0\\ \omega_{n,\chi}^2\end{bmatrix}\chi_{\text{err}}$

Close-in	$\chi_{\text{rstr}} = K_{P_\chi}\chi_{\text{err}} + K_{I_\chi}\int_0^t \chi_{\text{err}}(\tau)d\tau + K_{D_\chi}\dot{\chi}_{\text{err}}$ $\gamma_{\text{rstr}} = K_{P_\gamma}\gamma_{\text{err}} + K_{I_\gamma}\int_0^t \gamma_{\text{err}}(\tau)d\tau + K_{D_\gamma}\dot{\gamma}_{\text{err}}$ $\dot{V}_{\text{rstr}} = K_V\left(V_{\text{ref}} + V_r - V_{\text{rstr}}\right) + K_r r$
$\mathbf{P}_{\text{rstr}}$	$\dot{x}_{\text{rstr}} = V_{t,\text{rstr}}\cos\chi_{\text{rstr}}\cos\gamma_{\text{rstr}}$ $\dot{y}_{\text{rstr}} = V_{t,\text{rstr}}\sin\chi_{\text{rstr}}\cos\gamma_{\text{rstr}}$ $\dot{z}_{\text{rstr}} = -V_{t,\text{rstr}}\sin\gamma_{\text{rstr}}$

The initial values of all the dynamic states (integrators) used in the controller design are summarized in Table 11.

Table 11. Integrator Initial Value Setting.

State	Nominal $t=0$	Prevention $t=t_p$	Arrest $t=t_a$	Restoration $t=t_r$
$\dot{\mathbf{P}}_{\text{nom}}$	$\mathbf{V}_{\text{trim}}$	$\dot{\mathbf{P}}_{\text{nom}}(t_p)$	$\mathbf{V}_{\text{sen}}(t_a)$	$\mathbf{V}_{\text{sen}}(t_r)$
$\mathbf{P}_{\text{nom}}$	$\mathbf{P}_{\text{trim}}$	$\mathbf{P}_{\text{nom}}(t_p)$	$\mathbf{P}_{\text{sen}}(t_a)$	$\mathbf{P}_{\text{sen}}(t_r)$
$\mathbf{P}_{\text{err}}$	0	$\int_0^{t_p}\mathbf{P}_{\text{err}}(\tau)$	0	0
$\dot{\mathbf{V}}_{\text{nom}}$	$\mathbf{A}_{b,\text{trim}}$	$\dot{\mathbf{V}}_{\text{nom}}(t_p)$	$\mathbf{A}_{b,\text{sen}}(t_a)$	$\mathbf{A}_{b,\text{sen}}(t_r)$
$\mathbf{V}_{\text{nom}}$	$\mathbf{V}_{\text{trim}}$	$\mathbf{V}_{\text{nom}}(t_p)$	$\mathbf{V}_{\text{sen}}(t_a)$	$\mathbf{V}_{\text{sen}}(t_r)$
$\mathbf{V}_{\text{err}}$	0	$\int_0^{t_p}\mathbf{V}_{\text{err}}(\tau)$	0	0
$\dot{\mathbf{\Gamma}}_{\text{nom}}$	$\mathbf{\Omega}_{\text{trim}}$	$\dot{\mathbf{\Gamma}}_{\text{nom}}(t_p)$	$\mathbf{\Omega}_{\text{sen}}(t_a)$	$\mathbf{\Omega}_{\text{sen}}(t_r)$
$\mathbf{\Gamma}_{\text{nom}}$	$\mathbf{\Gamma}_{\text{trim}}$	$\mathbf{\Gamma}_{\text{nom}}(t_p)$	$\mathbf{\Gamma}_{\text{sen}}(t_a)$	$\mathbf{\Gamma}_{\text{sen}}(t_r)$
$\mathbf{\Gamma}_{\text{err}}$	0	$\int_0^{t_p}\mathbf{\Gamma}_{\text{err}}(\tau)$	0	0
$\dot{\mathbf{\Omega}}_{\text{nom1}}$	Θ_{trim}	$\dot{\mathbf{\Omega}}_{\text{nom1}}(t_p)$	$\Theta_{\text{sen}}(t_a)$	$\Theta_{\omega,\text{sen}}(t_r)$
$\mathbf{\Omega}_{\text{nom1}}$	$\mathbf{\Omega}_{\text{trim}}$	$\mathbf{\Omega}_{\text{nom1}}(t_p)$	$\mathbf{\Omega}_{\text{sen}}(t_a)$	$\mathbf{\Omega}_{\text{sen}}(t_r)$
$\mathbf{\Omega}_{\text{err1}}$	0	$\int_0^{t_p}\mathbf{\Omega}_{\text{err1}}(\tau)$	0	0
$\dot{\mathbf{\Lambda}}_{\text{nom}}$	0	$\dot{\mathbf{\Lambda}}_{\text{nom}}(t_p)$	0	0
$\mathbf{\Lambda}_{\text{nom}}$	$\mathbf{\Lambda}_{\text{sen}}(0)$	$\mathbf{\Lambda}_{\text{nom}}(t_p)$	$\mathbf{\Lambda}_{\text{arst}}(t_a)$	$\mathbf{\Lambda}_{\text{sen}}(t_r)$
$\mathbf{\Lambda}_{\text{err}}$	0	$\int_0^{t_p}\mathbf{\Lambda}_{\text{err}}(\tau)$	0	0
$\dot{\mathbf{\Omega}}_{\text{nom2}}$	0	$\dot{\mathbf{\Omega}}_{\text{nom2}}(t_p)$	$\Theta_{\text{arst}}(t_a)$	$\Theta_{\omega,\text{sen}}(t_r)$
$\mathbf{\Omega}_{\text{nom2}}$	0	$\mathbf{\Omega}_{\text{nom2}}(t_p)$	$\mathbf{\Omega}_{\text{arst}}(t_a)$	$\mathbf{\Omega}_{\text{sen2}}(t_r)$
$\mathbf{\Omega}_{\text{err2}}$	0	$\int_0^{t_p}\mathbf{\Omega}_{\text{err2}}(\tau)$	0	0
χ_{err}	0	0	$\int_{t_p}^{t_a}\chi_{\text{err}}(\tau)d$	$\int_{t_a}^{t_r}\chi_{\text{err}}(\tau)$
γ_{err}	0	0	$\int_{t_p}^{t_a}\gamma_{\text{err}}(\tau)$	$\int_{t_a}^{t_r}\gamma_{\text{err}}(\tau)$

V_{rstr}	V_{trim}	$V_{sen}(t_p)$	$V_{sen}(t_a)$	$V_{sen}(t_r)$
$\mathbf{P}_{rstr}$	$\mathbf{P}_{trim}$	$\mathbf{P}_{sen}(t_p)$	$\mathbf{P}_{sen}(t_a)$	$\mathbf{P}_{sen}(t_r)$

[00106] It will be appreciated that each of the modes described herein may be used independently or together in any combination as part of a flight management system. For example, the LOC prevention control, LOC arrest control, and nominal flight restoration control modes may be incorporated into a flight management system having a different baseline controller than the modified TLC 6DOF controller described herein. In another embodiment, the flight management system may not include a nominal flight restoration control mode and may instead rely on the pilot to restore the aircraft to its intended flight path.

[00107] While the present invention has been illustrated by the description of one or more embodiments thereof, and while the embodiments have been described in considerable detail, they are not intended to restrict or in any way limit the scope of the appended claims to such detail. Additional advantages and modifications will readily appear to those skilled in the art. The invention in its broader aspects is therefore not limited to the specific details, representative apparatus and method and illustrative examples shown and described. Accordingly, departures may be made from such details without departing from the scope or spirit of the general inventive concept.

WHAT IS CLAIMED IS:

1. An integrated loss-of-control prevention and recovery automatic control system of a fixed-wing aircraft comprising:

a plurality of flight control modes, including:

a nominal flight control mode;

a loss-of-control prevention control mode;

a loss-of-control arrest control mode; and

a nominal flight restoration control mode; and

a supervisory control system capable of monitoring the flight states and flight events of the aircraft and determining which flight control mode to activate.

2. The control system of claim 1, wherein the nominal flight control mode is defined by a six degree-of-freedom trajectory tracking controller with the wind-triangle and the post-stall aerodynamic characteristics in the calculation of the aerodynamic forces, and the time-varying parallel differential eigenvalues implemented in the feedback control gain matrices per Eqs. (9)-(11).

3. The control system of claim 1, wherein the loss-of-control prevention control mode includes a bandwidth adaptation to the nominal flight control mode to prevent a loss of control of the aircraft.

4. The control system of claim 3, wherein the loss-of control prevention control mode employs time-varying parallel differential eigenvalues to sacrifice tracking performance to increase capability of tolerance for severe wind and other abnormalities in real-time.

5. The control system of claim 1, wherein the loss-of-control prevention control mode augments the six degree-of-freedom trajectory tracking controller in the nominal flight control mode via the gain matrices per Eqs. (9)-(11).

6. The control system of claim 1, wherein the loss-of-control arrest control mode includes a full throttle control during an arrest phase.

7. The control system of claim 1, wherein the loss-of-control arrest control mode includes a commanded aerodynamic attitude determined by a level and straight flight trim value of angle-of-attack and zero sideslip and bank angles.

8. The control system of claim 7, wherein the loss-of-control arrest control mode tracks the commanded aerodynamic profile via inner and outer aerodynamic attitude loops.

9. The control system of claim 1, wherein the restoration mode includes a close-in sub-mode for guiding the aircraft to catch up with a target position dictated by a mission trajectory and a home-in sub-mode for restoring the mission trajectory of the aircraft.

10. The control system of claim 9, wherein the close-in sub-mode is defined by a guidance approach wherein a velocity vector of the aircraft is aligned to a line-of-sight vector of the aircraft using proportional-integral-derivative linear regulation in an Earth reference frame.

11. The control system of claim 9, wherein the home-in sub-mode includes a bandwidth adaptation for gradually regaining tracking performance of the aircraft and restoring the mission trajectory of the aircraft.

12. The control system of claim 1, wherein the supervisory control system includes a supervisory control logic variable having a value set according to flight states and flight events of the aircraft, and determining which flight control mode to activate..

13. The control system of claim 12, wherein the supervisory control logic variable is set to a value corresponding to the nominal flight control mode when a predetermined set of flight states of the aircraft are each within a predetermined set of operation thresholds.

14. The control system of claim 12, wherein the supervisory control logic variable is set to a value corresponding to the loss-of-control prevention control mode when at least one the flight states of the aircraft is within a predetermined set of protection thresholds.

15. The control system of claim 12, wherein the supervisory control logic variable is set to a value corresponding to the loss-of-control arrest control mode when at least one the flight states of the aircraft exceeds a predetermined set of safety thresholds.

16. The control system of claim 12, wherein the supervisory control logic variable is set to a value corresponding to the nominal flight restoration control mode when a predetermined set of flight states of the aircraft are each within a predetermined set of operation thresholds and a position error between the aircraft and a target position exceeds a range threshold.

17. A method of preventing loss-of-control of a fixed-wing aircraft having an automatic control system, comprising:

monitoring a plurality of flight states of the aircraft;

engaging a nominal flight control mode of the automatic control system when a predetermined set of flight states of the aircraft are each within a predetermined set of operation thresholds;

engaging a prevention mode of the automatic control system when at least one the flight states of the aircraft is within a predetermined set of protection thresholds; and

engaging a loss-of-control arrest mode of the automatic control system when at least one the flight states of the aircraft exceeds a predetermined set of safety thresholds.

18. The method of claim 17, further comprising:

engaging a restoration mode of the automatic control system when a predetermined set of flight states of the aircraft are each within a predetermined set of operation thresholds and a position error between the aircraft and a target position exceeds a range threshold.

19. An integrated loss-of-control prevention and recovery automatic control system of a fixed-wing aircraft comprising:

a plurality of flight control modes, including:

a nominal flight control mode; and

a loss-of-control prevention control mode; and

a supervisory control system capable of monitoring the flight states and flight events of the aircraft and determining which flight control mode to activate.

20. An integrated loss-of-control prevention and recovery automatic control system of a fixed-wing aircraft comprising:

a plurality of flight control modes, including:

a nominal flight control mode; and

a loss-of-control arrest control mode; and

a supervisory control system capable of monitoring the flight states and flight events of the aircraft and determining which flight control mode to activate.

21. A restoration mode for afixed-wing aircraft, comprising:

a close-in sub-mode for guiding the aircraft to catch up with a target position, wherein the close-in sub-mode is defined by a guidance approach wherein a velocity vector of the aircraft is aligned to a line-of-sight vector of the aircraft using proportional-integral-derivative linear regulation in an Earth reference frame; and

a home-in sub-mode for restoring a mission of the aircraft, wherein the home-in sub-mode includes a bandwidth adaptation for gradually regaining tracking performance of the aircraft and restoring the mission trajectory of the aircraft.

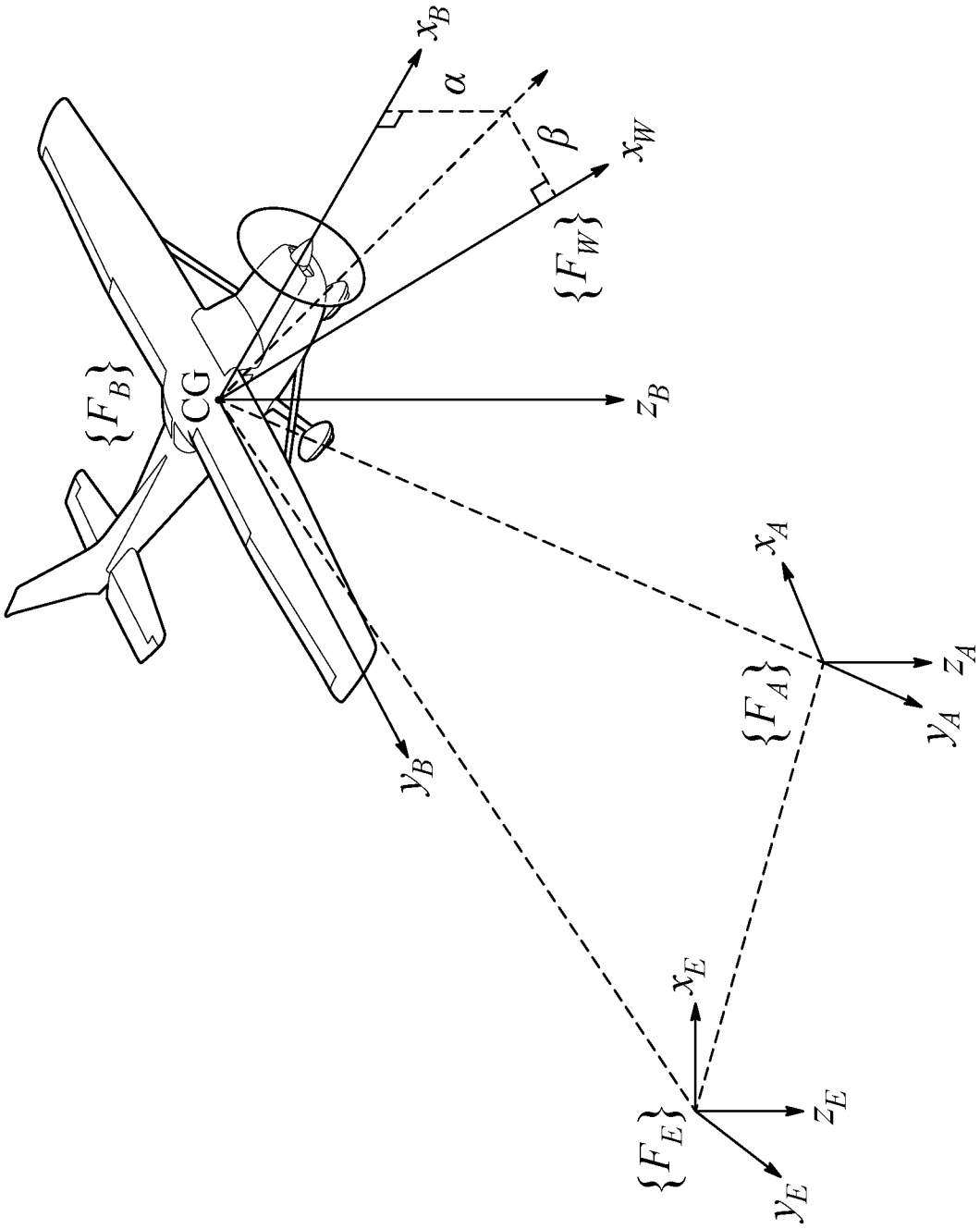


FIG. 1

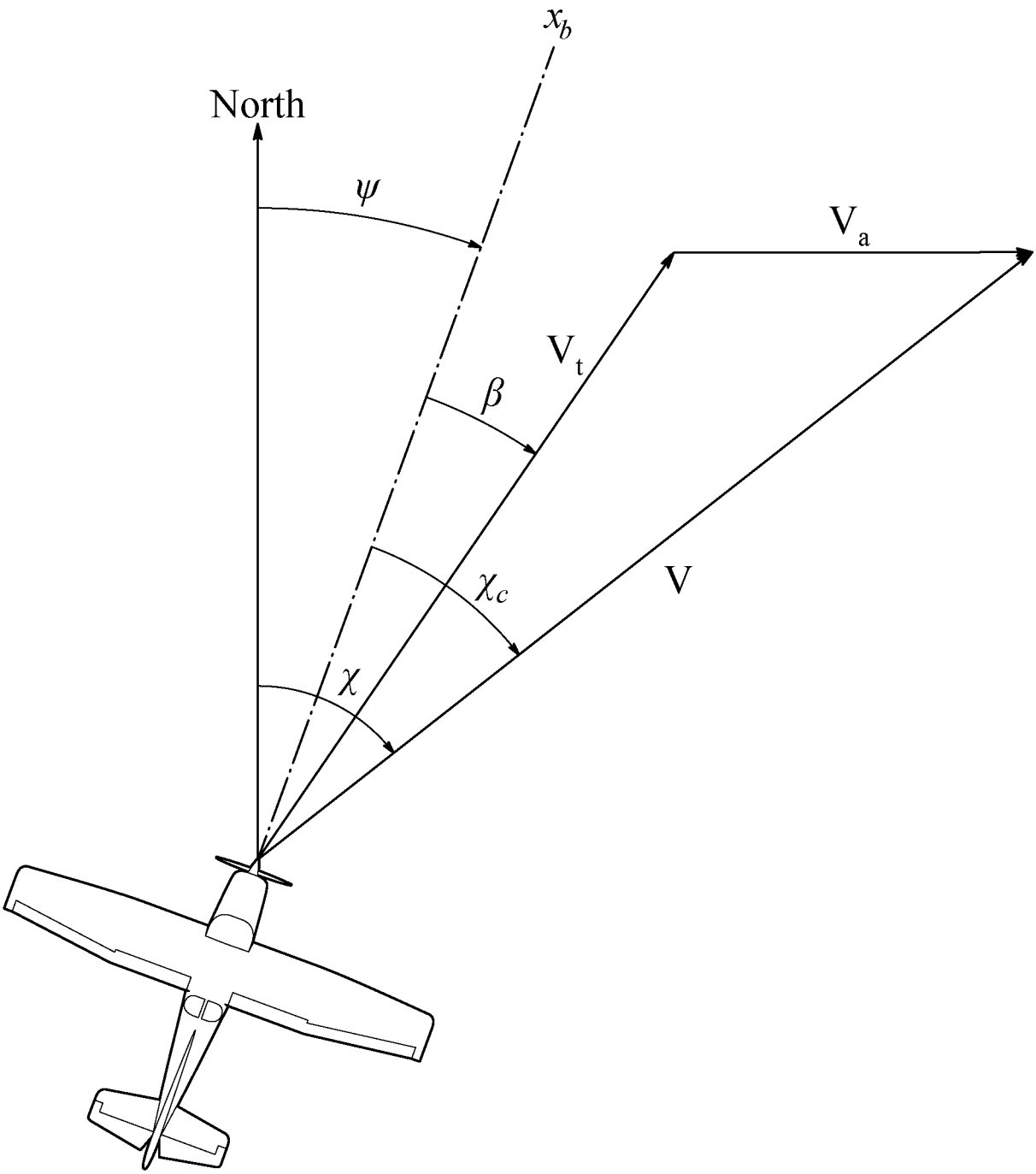


FIG. 2A

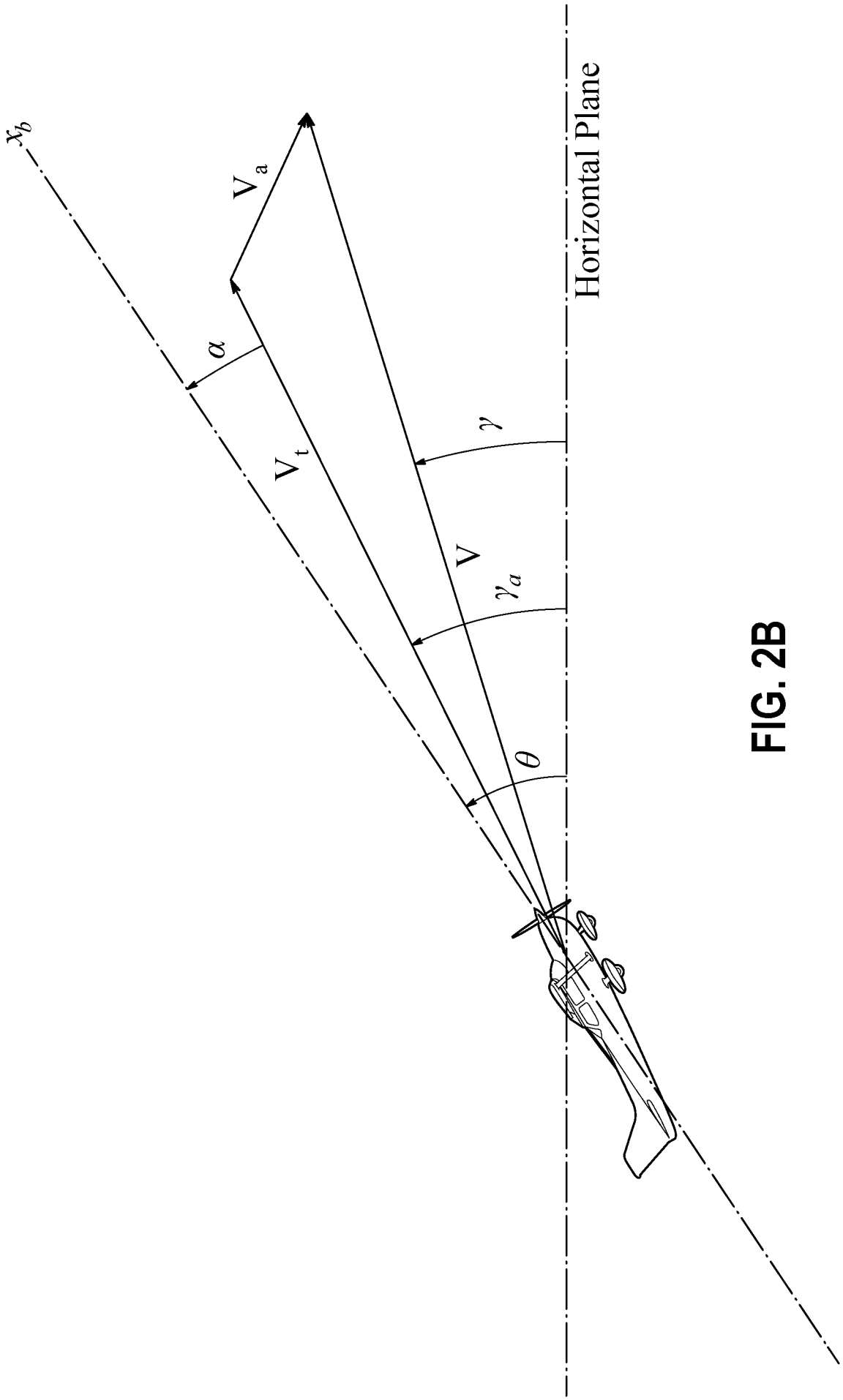


FIG. 2B

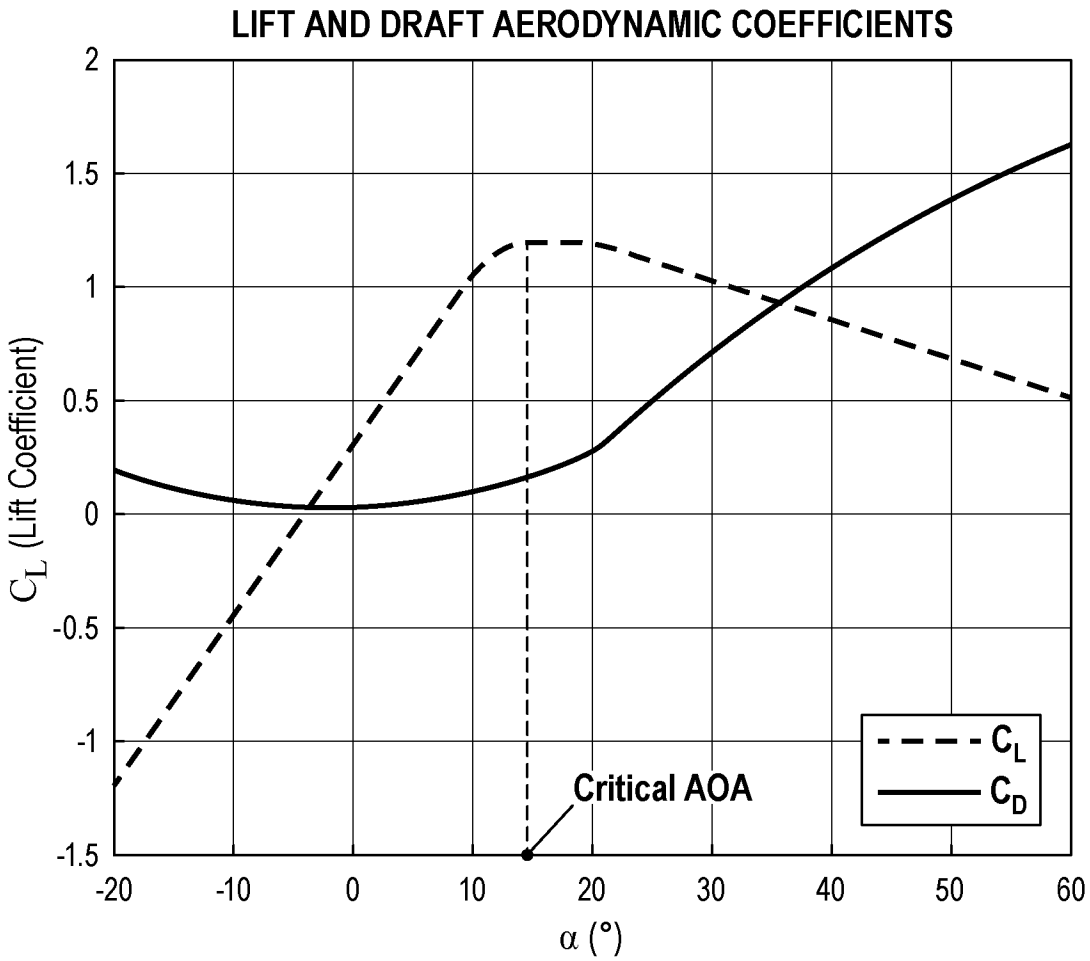

LIFT AND DRAFT AERODYNAMIC COEFFICIENTS
2
1.5
1
0.5
0
-0.5
-1
-1.5
C_L (Lift Coefficient)
-20
-10
0
10
20
30
40
50
60
α (°)
Critical AOA
C_L
C_D

FIG. 3

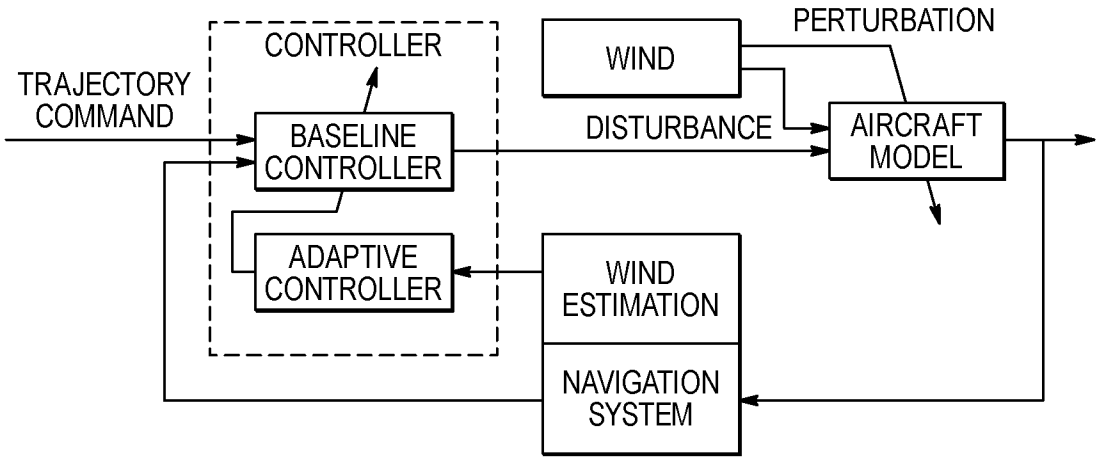

CONTROLLER
TRAJECTORY COMMAND
BASELINE CONTROLLER
ADAPTIVE CONTROLLER
WIND
PERTURBATION
DISTURBANCE
AIRCRAFT MODEL
WIND ESTIMATION
NAVIGATION SYSTEM

FIG. 4

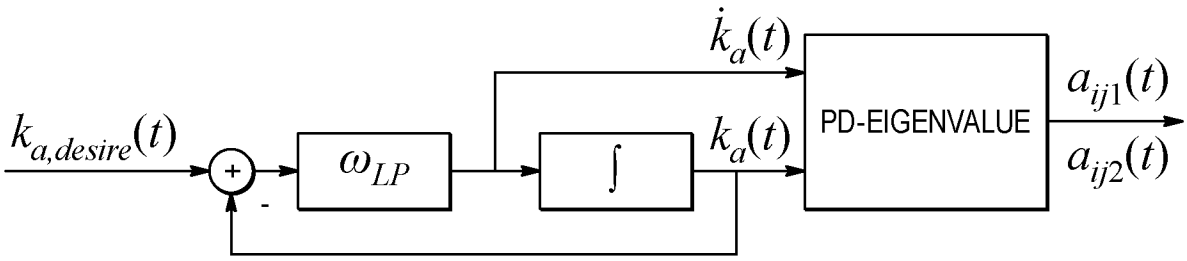

$\dot{k}_a(t)$
$k_{a,desire}(t)$
+
-
ω_{LP}
$\int$
$k_a(t)$
PD-EIGENVALUE
$a_{ij1}(t)$
$a_{ij2}(t)$

FIG. 5

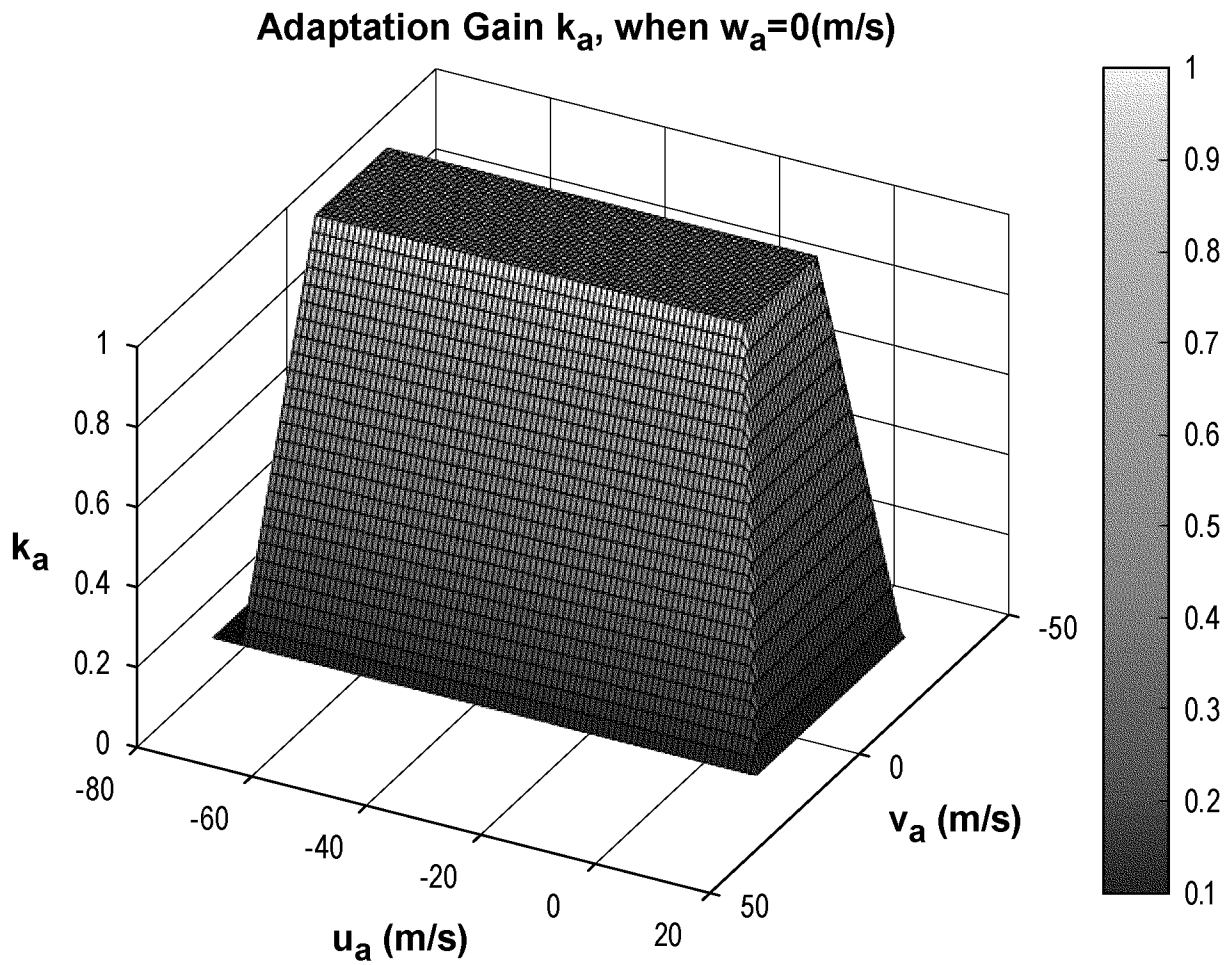

Adaptation Gain k_a, when w_a=0(m/s)
k_a
1
0.8
0.6
0.4
0.2
0
-80
-60
-40
-20
0
20
u_a (m/s)
50
0
-50
v_a (m/s)
1
0.9
0.8
0.7
0.6
0.5
0.4
0.3
0.2
0.1

FIG. 6

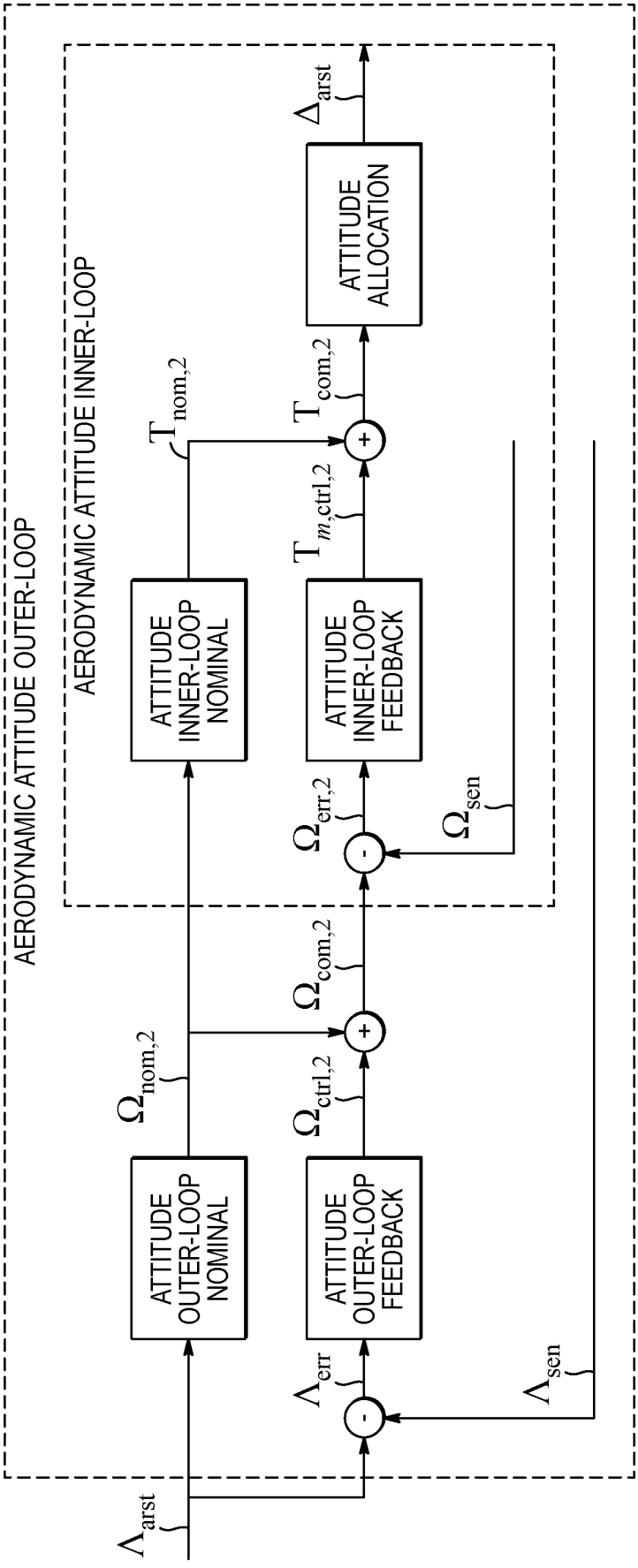

AERODYNAMIC ATTITUDE OUTER-LOOP
AERODYNAMIC ATTITUDE INNER-LOOP
ATTITUDE OUTER-LOOP NOMINAL
ATTITUDE OUTER-LOOP FEEDBACK
ATTITUDE INNER-LOOP NOMINAL
ATTITUDE INNER-LOOP FEEDBACK
ATTITUDE ALLOCATION
Λ_{arst}
Λ_{err}
Λ_{sen}
$\Omega_{nom,2}$
$\Omega_{ctrl,2}$
$\Omega_{com,2}$
$\Omega_{err,2}$
Ω_{sen}
$T_{nom,2}$
$T_{m,ctrl,2}$
$T_{com,2}$
Δ_{arst}

FIG. 7

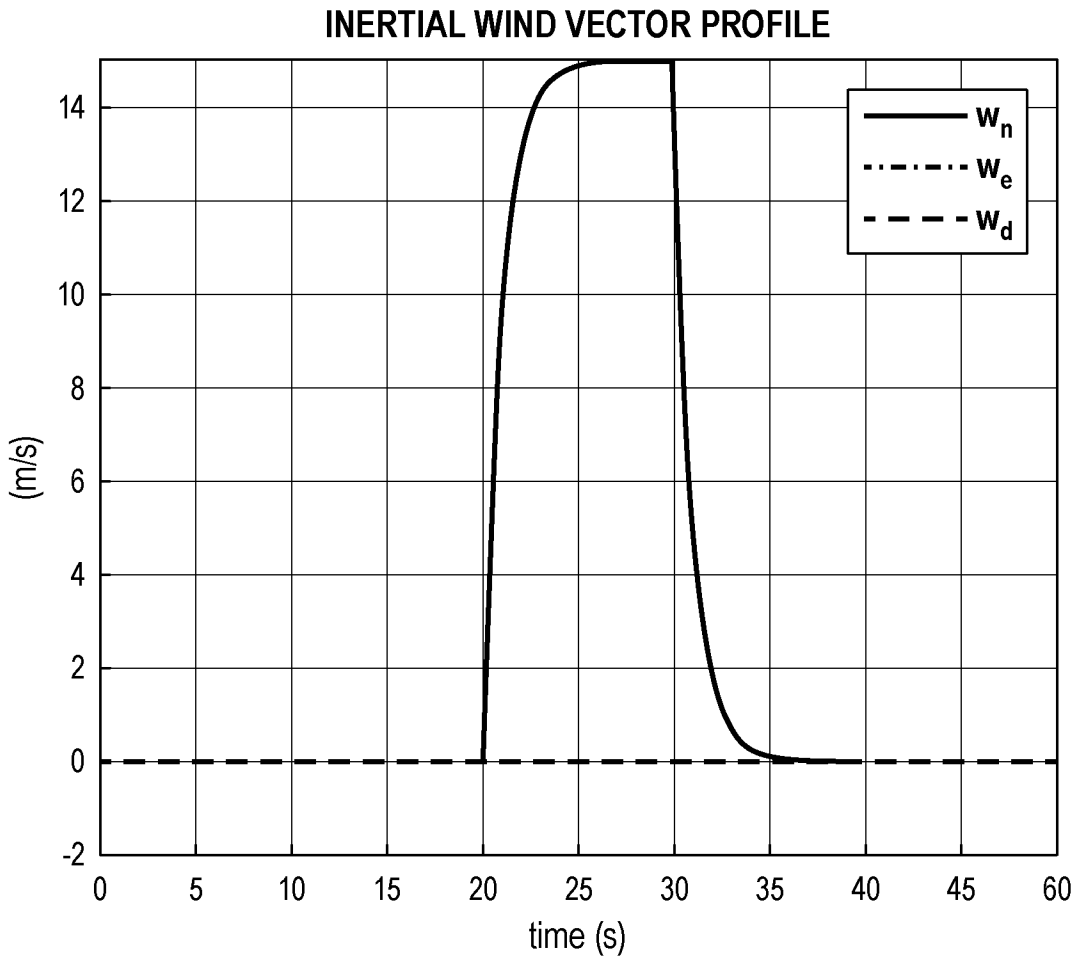

INERTIAL WIND VECTOR PROFILE
14
12
10
8
6
4
2
0
-2
(m/s)
0
5
10
15
20
25
30
35
40
45
60
time (s)
w_n
w_e
w_d

FIG. 8

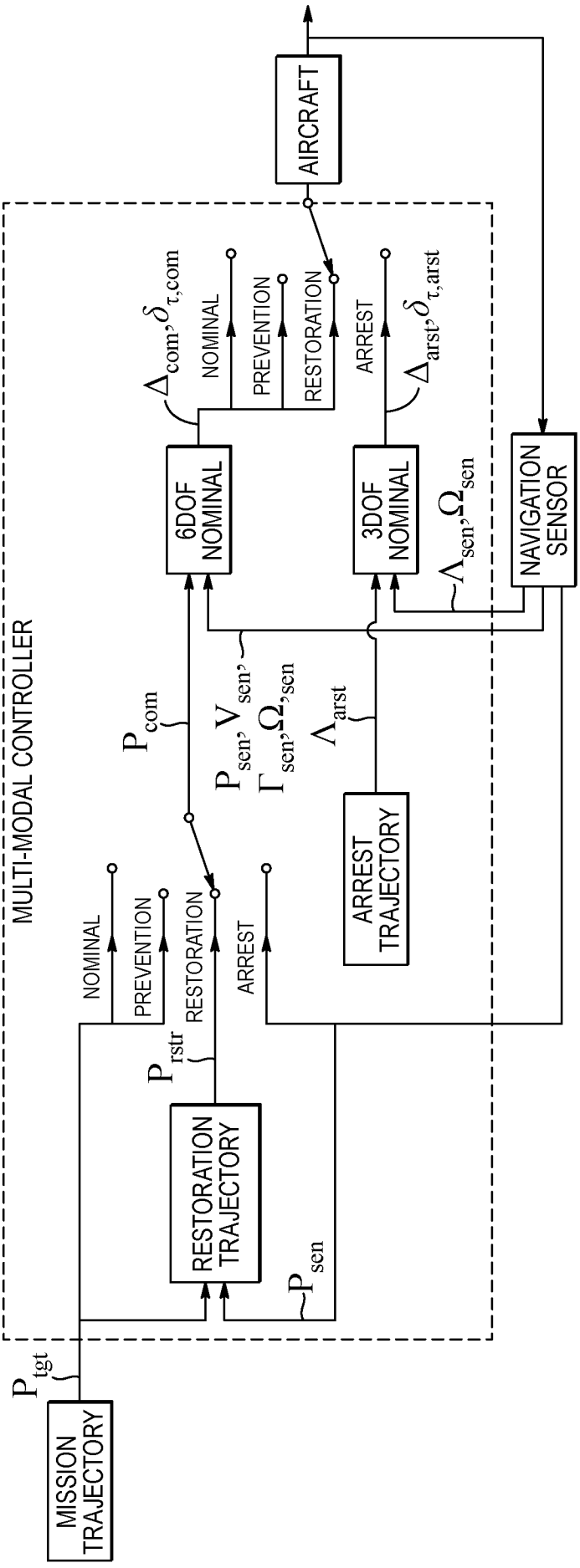

MISSION TRAJECTORY
P_{tgt}
MULTI-MODAL CONTROLLER
NOMINAL
PREVENTION
RESTORATION
ARREST
P_{rstr}
RESTORATION TRAJECTORY
P_{sen}
P_{com}
$P_{sen}, V_{sen},$
$\Gamma_{sen}, \Omega_{sen}$
Λ_{arst}
ARREST TRAJECTORY
6DOF NOMINAL
3DOF NOMINAL
$\Delta_{com}, \delta_{\tau,com}$
$\Delta_{arst}, \delta_{\tau,arst}$
$\Lambda_{sen}, \Omega_{sen}$
NAVIGATION SENSOR
AIRCRAFT

FIG. 9

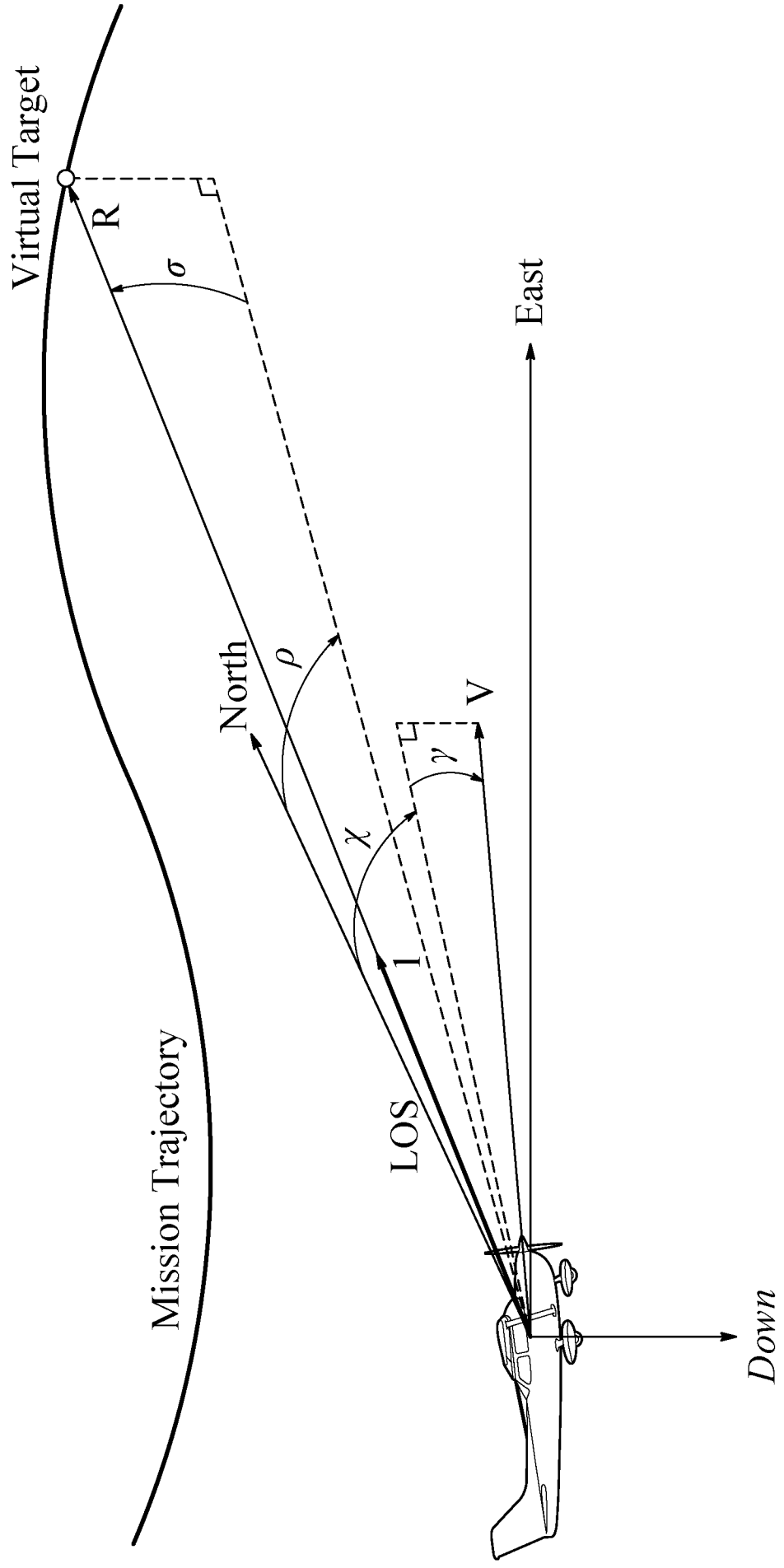

Virtual Target
R
σ
East
North
ρ
V
γ
χ
l
LOS
Mission Trajectory
Down

FIG. 10

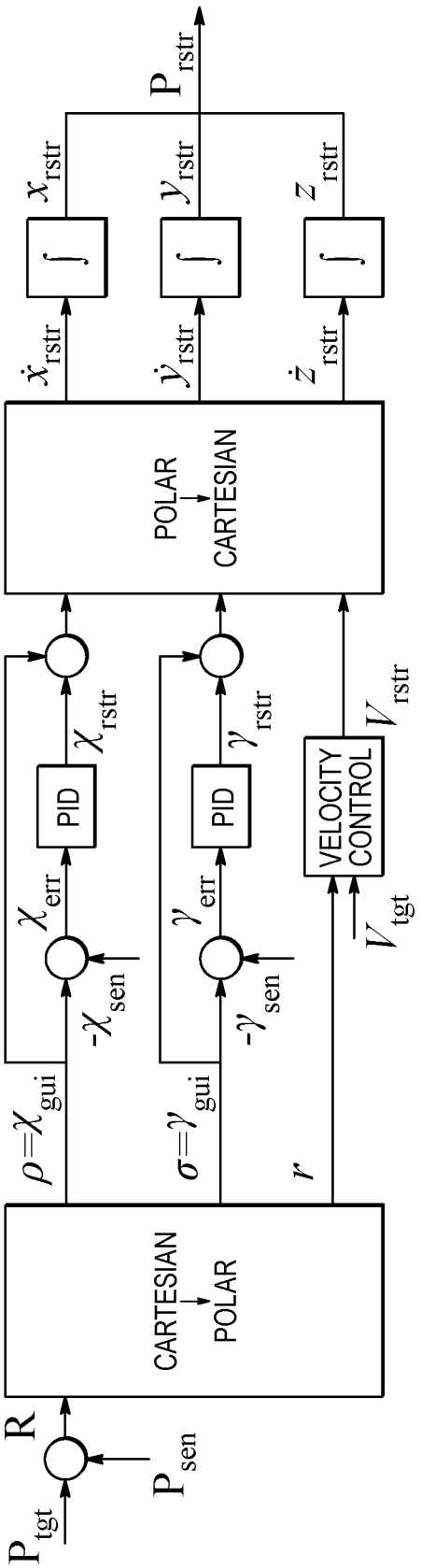

P tgt
R
P sen
CARTESIAN
POLAR
ρ=χ gui
σ=γ gui
r
-χ sen
-γ sen
χ err
γ err
PID
PID
χ rstr
γ rstr
VELOCITY CONTROL
V rstr
V tgt
POLAR
CARTESIAN
ẋ rstr
ẏ rstr
ż rstr
∫
∫
∫
x rstr
y rstr
z rstr
P rstr

FIG. 11

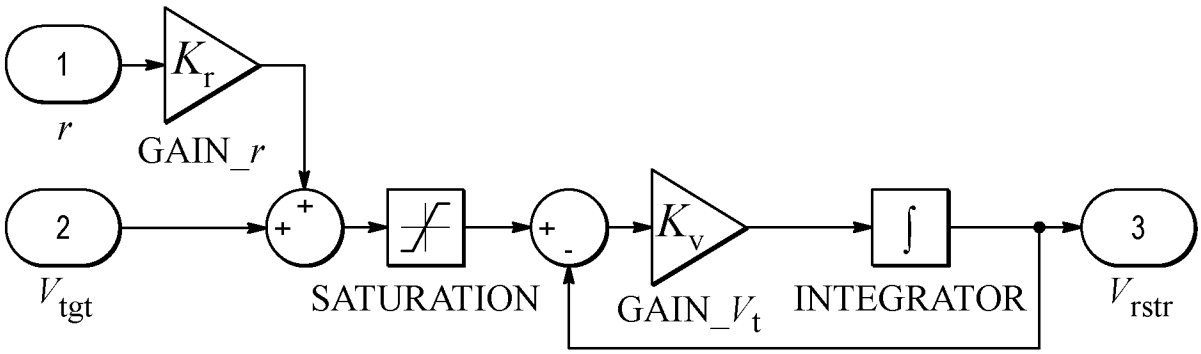


FIG. 12

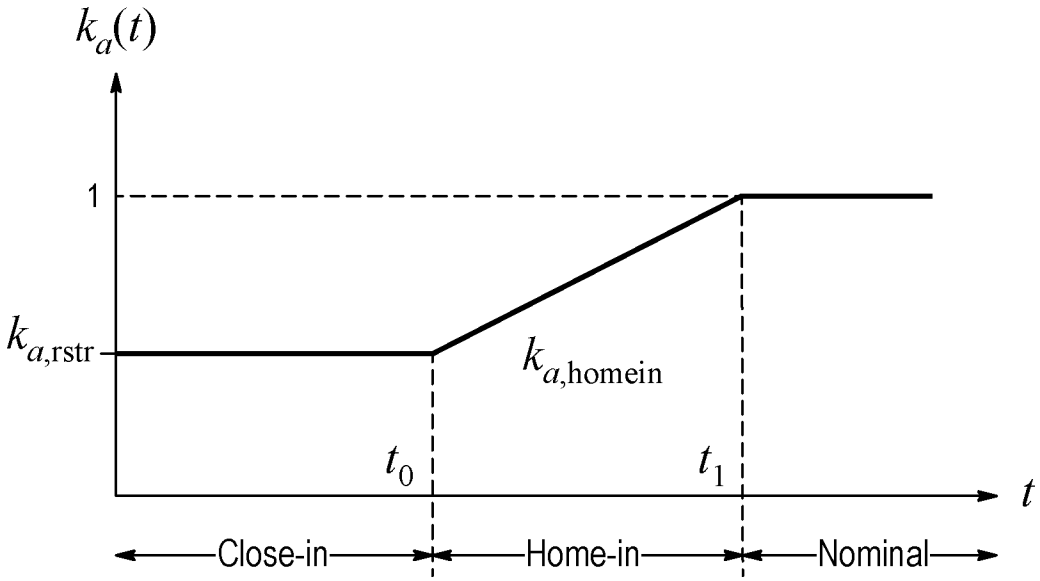


FIG. 13

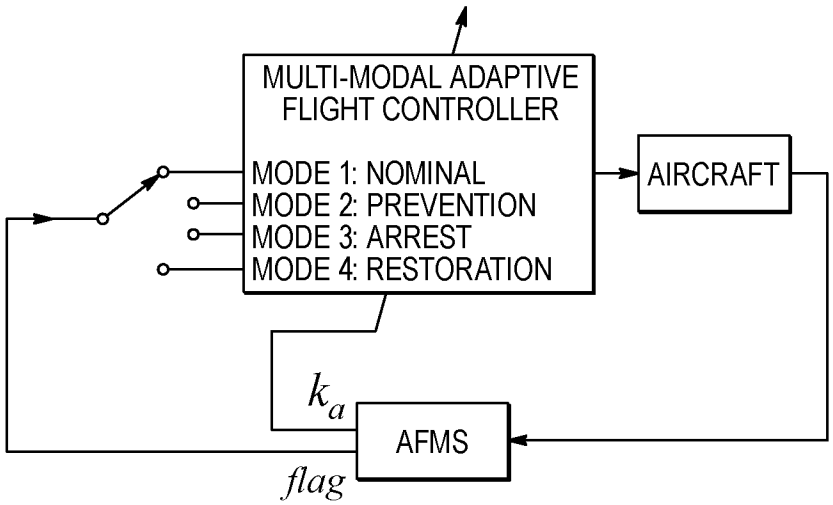


FIG. 14

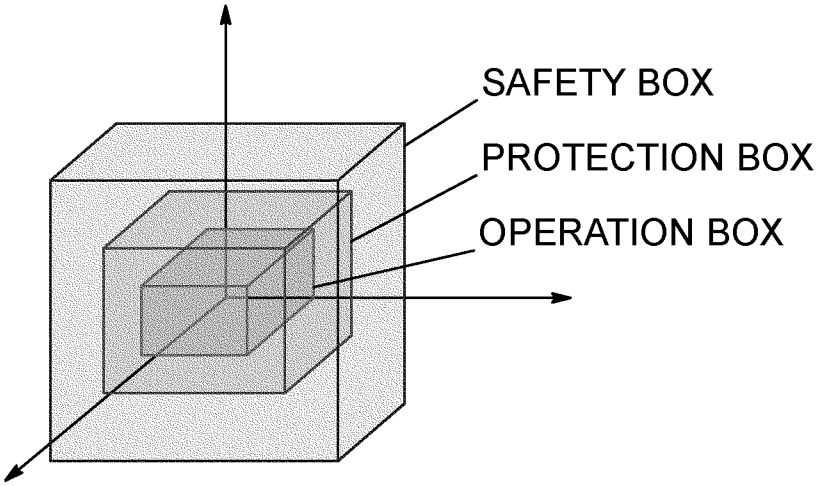

SAFETY BOX
PROTECTION BOX
OPERATION BOX

FIG. 15

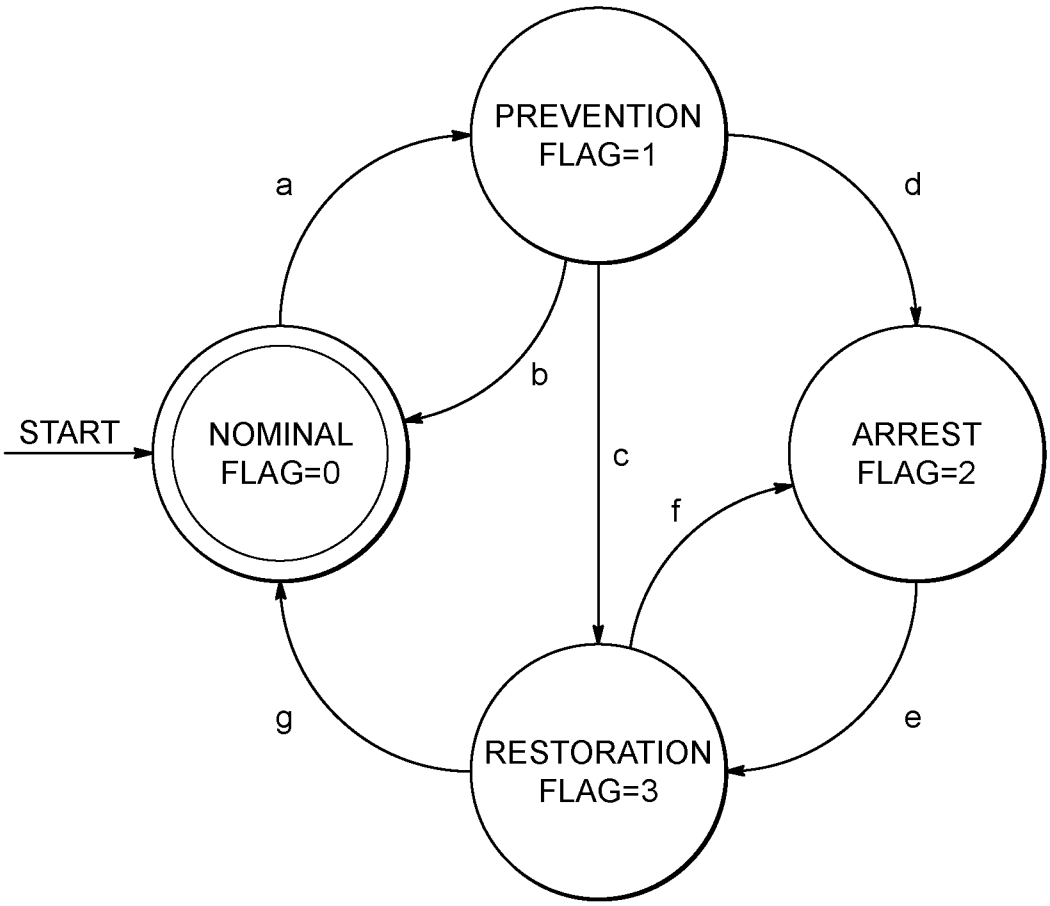

PREVENTION
FLAG=1
a
d
b
START
NOMINAL
FLAG=0
c
ARREST
FLAG=2
f
g
e
RESTORATION
FLAG=3

FIG. 16

INTERNATIONAL SEARCH REPORT

International application No.
PCT/US 16/53030

A. CLASSIFICATION OF SUBJECT MATTER
IPC(8) - G01C 23/00 (2016.01)
CPC - G01C 23/00
According to International Patent Classification (IPC) or to both national classification and IPC

B. FIELDS SEARCHED

Minimum documentation searched (classification system followed by classification symbols)
IPC(8): G01C 23/00 (2016.01);
CPC: G01C 23/00

Documentation searched other than minimum documentation to the extent that such documents are included in the fields searched
USPC: 701/3, 701/14; IPC(8): G01C 23/00 (2016.01);
CPC: G01C 23/00, G08G 5/0021, G01C 23/005, G08G 5/0013, G08G 5/0052

Electronic data base consulted during the international search (name of data base and, where practicable, search terms used)
PatBase, ProQuest Dialog, Google Web, Google Patents (Search terms: loss, control, arrest mode, land, brake, decelerate, aircraft, prevent, inhibit, flight modes, nominal, restore, parallel differential eigenvalue, bandwidth adaptation, line-of-sight, align, vector, proportional integral derivative, threshold, close-in, guide, home-in, track, etc.)

C. DOCUMENTS CONSIDERED TO BE RELEVANT

Category*	Citation of document, with indication, where appropriate, of the relevant passages	Relevant to claim No.
Y	US 2014/0371957 A1 (Riedinger et al.) 18 December 2014 (18.12.2014), para. [0037], [0075], [0083], [0092]-[0093], [0137]-[0138], [0156], [0167]-[0168], and [0170], and Fig. 10, and Table 1.	1-20
Y	US 2005/0230566 A1 (A'Harrah) 20 October 2005 (20.10.2005), para. [0031] and [0038]-[0039].	1-19
Y	US 2015/0183510 A1 (Vander Lind et al.) 02 July 2015 (02.07.2015), para. [0080], [0088], [0095], and [0166].	1-18, 20
Y	US 2015/0197335 A1 (Dekel et al.) 16 July 2015 (16.07.2015), para. [0089], [0093], [0095], [0115], and [0416].	9-11, 21
Y	US 2011/0043786 A1 (Lacondemine et al.) 24 February 2011 (24.02.2011), para. [0067].	10, 21
Y	US 4,212,443 A (Duncan et al.) 15 July 1980 (15.07.1980), col. 5 ln. 15-16 and 23-34.	3-4, 9-11, 21
Y	US 2012/0095621 A1 (Zhu et al.) 19 April 2012 (19.04.2012), para. [0095], [0101]-[0102], and [0105], and Equations 6-8	2, 4-5, 8

☐ Further documents are listed in the continuation of Box C. ☐

* Special categories of cited documents:
"A" document defining the general state of the art which is not considered to be of particular relevance
"E" earlier application or patent but published on or after the international filing date
"L" document which may throw doubts on priority claim(s) or which is cited to establish the publication date of another citation or other special reason (as specified)
"O" document referring to an oral disclosure, use, exhibition or other means
"P" document published prior to the international filing date but later than the priority date claimed
"T" later document published after the international filing date or priority date and not in conflict with the application but cited to understand the principle or theory underlying the invention
"X" document of particular relevance; the claimed invention cannot be considered novel or cannot be considered to involve an inventive step when the document is taken alone
"Y" document of particular relevance; the claimed invention cannot be considered to involve an inventive step when the document is combined with one or more other such documents, such combination being obvious to a person skilled in the art
"&" document member of the same patent family

Date of the actual completion of the international search	Date of mailing of the international search report
22 November 2016 (22.11.2016)	15 DEC 2016
Name and mailing address of the ISA/US Mail Stop PCT, Attn: ISA/US, Commissioner for Patents P.O. Box 1450, Alexandria, Virginia 22313-1450 Facsimile No. 571-273-8300	Authorized officer: Lee W. Young PCT Helpdesk: 571-272-4300 PCT OSP: 571-272-7774

Form PCT/ISA/210 (second sheet) (January 2015)